DUCTILE FRACTURE ANALYSIS IN A STEEL PLATE

BY COHESIVE ZONE MODELING

by

© Tayyebe Seif

A Thesis submitted to the

School of Graduate Studies

in partial fulfillment of the requirements for the degree of

Master of Engineering

Faculty of Engineering and Applied Science

Memorial University of Newfoundland

July 2014

St. John's Newfoundland and Labrador Canada

ABSTRACT

There are several theories used to describe fracture process including Linear Elastic Fracture Mechanics (LEFM), Elastic-Plastic Fracture Mechanics (EPFM), and Cohesive Zone Models (CZM), which allow for development of predictive capabilities. The main disadvantage of LEFM and EPFM techniques is that only structures with an initial crack can be modeled. Other drawbacks of these techniques are geometry dependence and validity limits. In contrast, CZM can simulate fracture in any structures, with or without a crack. CZM is not confined to a class of materials, but it can be used for arbitrary materials.

In this research, the CZM was used to numerically simulate crack initiation and growth in steel plates. Within the CZM, material separation (i.e. damage of the structure) is described by interface elements, which open irreversibly and lose their stiffness at failure, causing the continuum elements to be disconnected. Numerical simulation of tensile tests was conducted to determine and validate the cohesive parameters and then these parameters were used for modeling mode I fracture in steel plates. It was shown that the cohesive model is capable of simulating ductile fracture in cases where the crack path is not known in advance and the crack can evolve anywhere in the specimen.

ACKNOWLEDGMENTS

I would like to express my gratitude to Dr. Claude Daley, my supervisor, and Dr. Bruce Colbourne, my co-supervisor, for their guidance and financial support during my graduate study, whose expertise, understanding, and patience, added considerably to my graduate experience.

I would also like to thank all my family, particularly my father, Mehdi Seif, for the love and the encouragement. The first Naval Architect Engineer I met and the reason I decided to be a Naval Architect Engineer one day. I will never be sufficiently thankful to my family for their constant support and encouragement.

Additionally, I must acknowledge that without my friend, my colleague, my husband, and my partner in crime, Abdullah Jamaly, I would not have been able to complete this project. He was always there when I needed his support. For all that he has done for me, this thesis is dedicated to him.

July 2014

St. John's

Table of Contents

List of Tables

List of Figures

List of Nomenclature

BK	Benzeggagh and Kenane mixed mode criterion
CZM	Cohesive Zone Model
EPFM	Elastic-Plastic Fracture Mechanics
FE	Finite Element
FEM	Finite Element Methods
FEA	Finite Element Analysis
GTN	Gurson–Tvergaard–Needleman
JR-curve	J-integral Resistance curve
LEFM	Linear Elastic Fracture Mechanics
SZW_c	Critical Stretch Zone Width
TSL	Traction-Separation Law

A	Crack area
Δa	Crack extension
E	Young's modulus
e	Engineering strain
ε	True strain
ε_p	Plastic strain
ε_e	Elastic strain
G	Energy release rate per unit crack front length
G_c	Fracture energy
G_I	Energy release rate per unit crack front length in mode I fracture

G_{IC}	Mode I fracture energy
G_{II}	Energy release rate per unit crack front length in mode II fracture
G_{IIC}	Mode II fracture energy
G_{III}	Energy release rate per unit crack front length in mode III fracture
G_{IIIC}	Mode III fracture energy
J	J-integral
J_i	J-integral at crack initiation
K	Stress intensity factor
K_c	Critical stress intensity factor
K_I	Critical stress intensity factor in mode I fracture
K_{II}	Critical stress intensity factor in mode II fracture
K_{III}	Critical stress intensity factor in mode III fracture
l_0	Gauge length of the tensile specimen
P	Normal force
T	Traction
T_0	Critical traction
T^T	Tangential traction
T_0^T	Critical tangential traction
T^N	Normal traction
T_0^N	Critical normal traction
u	Displacement
u^+	Displacement of the upper node
u^-	Displacement of the lower node

U	Potential energy
η	Stress triaxiality
Γ	Surface energy
Γ_0	Critical surface energy / Fracture energy
Γ_0^N	Normal fracture energy
Γ_0^T	Tangential fracture energy
ν	Poisson's ratio
σ_y	yield strength
σ_U	Maximum tensile strength
σ_H	Hydrostatic stress
σ_{eq}	Von Mises equivalent stress
σ_T	True stress
σ_E	Engineering stress
δ	Separation
δ_0	Critical separation
δ^N	Normal separation
δ_0^N	Critical normal separation
δ^T	Tangential separation
δ_0^T	Critical tangential separation

Chapter 1: Introduction

1-1. Introduction

Due to the substantial increase in oil and gas activities in the Arctic, the demand for ice strengthened vessels has increased greatly. This increase in demand has highlighted the importance of designing ice strengthened ship structures that maintain adequate safety and integrity. In order to meet these new challenges, reliable prediction of the ultimate strength of a structure is essential.

Traditionally, ship structures were designed to prevent yielding failure. However, steel has very great reserve strength after it yields and before it finally collapses, which is an advantage for cases when ship structures need to absorb large impact energy, such as in an ice-structure accident. The use of some portion of the reserve capacity for resisting loads will result in lighter structures, which are easier to fabricate and more economical. Using this reserve capacity causes a challenge to the balance between safety needs and commercial flexibility. Hence, investigating the ultimate strength of the structure is crucial.

One of the main concerns in collision events is fracture in the outer hull. Once fracture occurs, the resistance to further damage drops dramatically. This may accelerate the hull opening process. Potential consequences are the risk of flooding and polluting the environment with fuel and cargo oil. With smaller damages, the ship's stability may not be affected, but leakage of oil and fuel may occur, threatening the environment. Hence, the simulation of the damage propagation and the crack growth can also be crucial beside the prediction of the crack initiation. In order to ensure the integrity of structures, it is essential to develop advanced models that are able to capture the failure mechanisms occurring in such structures.

Since steel plates are the basic structural elements in many ships and offshore structures, understanding of the steel plate behavior is essential. The behavior of steel in the elastic region is well understood. In recent years, there has been a new interest in estimating the plastic response and the ultimate strength (failure capacity) of the structure, in order to use some portion of the reserve capacity of the structure in specific cases that seem economically rational.

"Sustainable Technology for Polar Ships and Structures" (STePS2), a project at the Faculty of Engineering and Applied Science at Memorial University of Newfoundland, focuses on developing design tools for polar ships and offshore structures. The aim of this study, as part of STePS2 project, is to gain a better understanding of the response of a steel plate to extreme ice load by exploring ductile fracture in steel plates numerically. Classical methods that are available to predict and evaluate fracture are discussed. Among them, recently developed method, Cohesive Zone Models (CZM), is chosen to simulate crack initiation and propagation numerically.

CZMs are able to describe materials that exhibit strain-softening type behaviour. The basic assumption underlying them is the formation of a fictitious crack, as an extension of the real crack, referred to also as the process zone, where the material is still able to transfer stresses, although it is damaged. The crack is assumed to propagate when the stress at the crack tip reaches the cohesive strength. When the crack opens, the stress is not assumed to fall to zero at once but to decrease gently with increasing crack width until a critical displacement is reached and the interaction vanishes.

The basic idea of the CZM is to split the material's behavior in deformation, which is modeled by continuum elements, and damage or separation, which is modeled by embedded interface elements within continuum elements. The material separation and thus damage of the structure is described by interface elements, no continuum elements are damaged in CZM. Using this technique, the behavior of the material is split in two parts, the damage-free continuum with an arbitrary material law, and the cohesive interfaces between the continuum elements, which specify only the damage of the material.

CZM, its application, advantages and disadvantages will be explained in detail in the following chapter. It will be presented that by investigating CZM to predict fracture initiation and propagation, it is possible to estimate the ship hull indentation resistance.

The topic of this thesis originated to investigate the field of fracture mechanics and related theories and methods. Its main goal is to develop a better understanding of how to use the finite element method to simulate ice-structure collision and the damage caused by ice. The focus of the thesis has been on the ductile fracture of metal, particularly steel, and the use of CZM for simulating ductile fracture in mode I.

This thesis gives an overview of the theory involved in a ductile failure of an isotropic ductile material such as steel, and explains CZM theory for modeling the material behavior related to ductile fracture for use in the finite element method. The cohesive material model is developed using tensile tests simulation in the finite element software ABAQUS. Then the developed material model is used to simulate fracture in steel plates being penetrated by a rigid indenter at low speed.

1-2. Fracture Mechanics

The relationship between the stress and the strain depends on the mechanical properties of the material, specifically on their deformation behavior. In Figure 1-1 the characteristic features of elastic-plastic behavior are presented by the stress-strain curve.

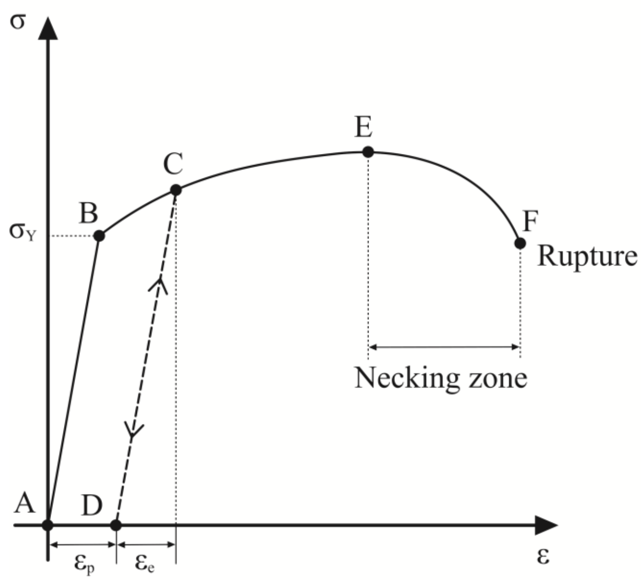

Figure 1-1: Elastic-plastic material behavior

The material behaves elastically until a certain stress value is reached at point B, the yield strength σ_y. Elastic material behavior is characterized by the feature that the deformations are reversible. The stress-strain relation is linear in the elastic range for most of materials, which is known as Hooke's law:

$$\sigma = E\varepsilon \qquad \text{Eq. (1-1)}$$

The modulus of elasticity (Young's modulus), E, is given by the slope of the stress-strain curve:

$$E = \frac{d\sigma}{d\varepsilon} \qquad \text{Eq. (1-2)}$$

If the stress exceeds σ_y, inelastic permanent deformations occur and plastic strains are formed, $\varepsilon_p > 0$. In real materials the current yield strength, σ_y, increases as a result of plastic deformation, which is denoted as hardening of the material. Plastic deformations are irreversible. If the applied stress is reduced to zero (point D in Figure 1-1), the material is relieved by a pure elastic deformation ε_e and only ε_p remains. After unloading, the plastic deformations remain. The plastic work of deformation is predominantly converted into heat.

The stress-strain relation is non-linear in the plastic region, but can be approximated as linear in the practical ranges of structural deformation. Thus the total stress-strain is normally approximated as a bilinear curve with linear hardening.

Beyond point E in Figure 1-1, there is a noticeable reduction of load-carrying capacity until rupture. The deformation during this last phase is localized in a neck region of the specimen. Point E identifies the material state at the onset of damage. Beyond this point, the stress-strain response is governed by the evolution of the degradation of the stiffness in the region of strain localization (EF in Figure 1-1, this region is called necking region). At Point F in Figure 1-1 rupture happens.

Fracture is the separation of an object or material. A detailed understanding of how fracture occurs in materials may be assisted by the study of fracture mechanics. The prediction of failure initiation and evolution are, in general, difficult. This is covered in fracture mechanics. Fracture mechanics specifically addresses the issue of whether a body under load will remain intact or whether a new free surface will form.

There are three independent loading modes to enable a crack to propagate (Figure 1-2):

- Mode I fracture- Opening mode where a tensile stress normal to the plane of the crack is applied and this is the most common load type.
- Mode II fracture- Sliding mode or in-plane shear mode where a shear stress acting parallel to the plane of the crack and perpendicular to the crack front.
- Mode III fracture- Tearing mode or out-of-plane shear mode where a shear stress acting parallel to the plane of the crack and parallel to the crack front.

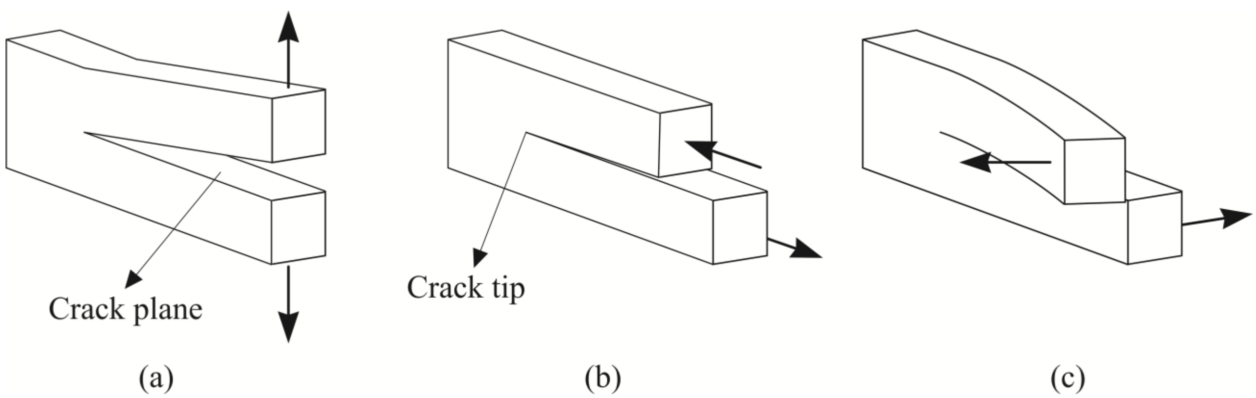

Figure 1-2: Fracture modes. a) Mode I, b) Mode II, c) Mode III

For engineering materials, such as metals, there are two primary modes of fracture: brittle and ductile. In brittle fracture cracks spread very rapidly with little or no plastic deformation. In brittle fracture, no apparent plastic deformation takes place before fracture. Cracks that initiate in a brittle material tend to continue to grow and increase in size provided the loading will cause crack growth.

In contrast, ductile fracture includes three stages: void nucleation, growth, and coalescence (Figure 1-3). Ductile fracture often occurs shortly after the onset of local necking, and relates to the formation of micro-voids which grow and eventually coalesce as the material is strained. In ductile fracture, extensive plastic deformation (necking) takes place before fracture. Some of the energy from stress concentrations at the crack tips is dissipated by plastic deformation before the crack actually propagates. The crack moves slowly and is accompanied by a large amount of plastic deformation. The crack typically will not grow unless the applied load is increased. Ductile fracture surfaces have larger necking regions and an overall rougher appearance than brittle fracture surfaces.

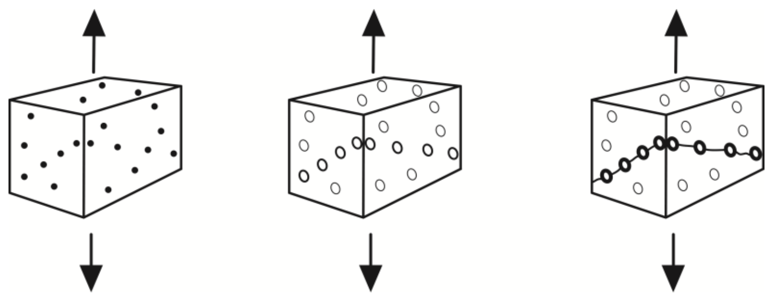

Figure 1-3: Void nucleation, growth, and coalescence in a ductile material (Based on Tornqvist, 2003)

Fracture surfaces and stress-strain curves for both ductile and brittle fracture are shown in Figure 1-4. Plastic deformation in ductile fracture can be seen in these figures.

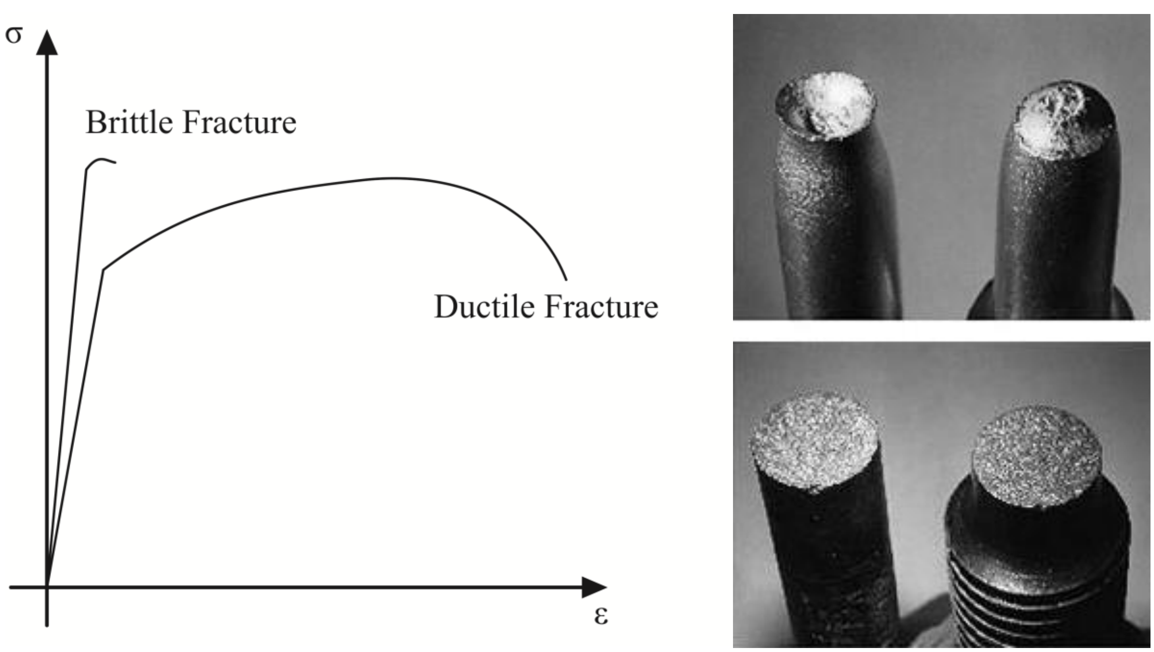

Figure 1-4: Ductile and brittle fracture

Fracture toughness is a property of a material which describes the ability of the material containing a crack to resist fracture, and is one of the most important properties of any material for many design applications. Fracture toughness is a quantitative way of expressing a material's resistance to brittle fracture when a crack is present. If a material has much fracture toughness, it will probably undergo ductile fracture. Brittle fracture is very characteristic of materials with less fracture toughness.

Whether fracture in a specific material is ductile or brittle can depend on the temperature of the environment. Steel is a typical example of dual behavior that shows brittle behavior at very low temperatures and is ductile at high temperatures. Generally, fracture toughness depends on temperature, loading rate, the composition of the material and its microstructure, together with the geometric effects of the crack tip.

The design process of a structure consists of choosing the appropriate material strength as per the loading conditions, and structural analysis, so that it does not fail under load. Different approaches exist to investigate damage, material separation and fracture phenomena in order to develop predictive capabilities, including Linear Elastic Fracture Mechanics (LEFM), Elastic-Plastic Fracture Mechanics (EPFM), and local approaches such as CZM. In the following an overview of these methods are presented.

1-2-1. Linear Elastic Fracture Mechanics

LEFM is the basic theory of fracture that deals with sharp cracks in elastic bodies and predicts whether a specific crack in the body will grow more or not. For linear elastic materials (i.e., brittle), LEFM characterizes the local crack tip stress field using a single parameter called the stress intensity factor, K. It is defined from the elastic stresses near the tip of a sharp crack under remote loading. K is used to predict the stress intensity near the tip of a crack and it is a method of calculating the amount of energy available for fracture around a crack front in a linear elastic material. When it becomes critical, the crack grows and the material fails. This critical value is denoted K_c and is known as the fracture toughness, which is a material property.

Energy principles play an important role in studying crack problems. This is motivated by the fact that crack propagation always involves dissipation of stress-strain energy. This energy is dissipated in process zone because of plastic deformation, formation of micro separations, and coalescences. Irwin (1957) was the first who observed that if the size of the plastic zone around crack tip is small compared to the size of the crack (i.e. in brittle materials), the energy required to grow the crack will not be critically dependent on the state of stress at the crack tip. According to this assumption, the energy needed to create a unit fracture surface which goes into the plastic deformation, the fracture process, and formation of new surfaces, is a constant that depends only on the material. This quantity is called fracture energy (G_c) and is considered to be a material property which is independent of applied loads and the geometry of the body. By considering fracture from an energy point of view, crack growth criteria can be expressed in terms of energy release rates. Crack propagation starts when the energy coming from the stress- strain field is suffcient to support the formation of micro voids and coalescences. Similar to K-based fracture criteria, the crack propagation starts when $G > G_c$.

This approach offers an alternative to the K-based fracture criteria discussed earlier and reinforces the connection between global and local fields in fracture problems. The energy release rate is a global parameter while the stress intensity factor is a local crack-tip parameter. Irwin showed that for a mode I crack the strain energy release rate and the stress intensity factor are related by:

$$G = -\frac{\partial U}{\partial A} = \frac{K_I^2}{E'} \qquad \text{Eq. (1-3)}$$

Where E' denotes the effective Young's modulus for plane stress or plane strain. For plane strain:

$$E' = \frac{E}{1-\nu^2} \qquad \text{Eq. (1-4)}$$

and for plane stress:

$$E' = E \qquad \text{Eq. (1-5)}$$

U is the potential energy available for crack growth and A is the crack area. E is the Young's modulus, ν is Poisson's ratio, and K_I is stress intensity factors in mode I fracture.

Irwin adopted the assumption that the size and shape of the energy dissipation zone remains approximately constant during brittle fracture. This assumption suggests that the energy needed to create a unit fracture surface is a constant that depends only on the material.

However, in ductile materials (and even in materials that appear to be brittle), a plastic zone develops at the tip of the crack. As the applied load increases, the plastic zone increases in size until the crack grows and the material behind the crack tip unloads. The plastic loading and unloading cycle near the crack tip leads to the dissipation of energy as heat. In physical terms, additional energy is needed for crack growth in ductile materials when compared to brittle materials.

In brittle materials, fracture energy and surface energy are equal, $G = \Gamma$ (Surface energy quantifies the disruption of intermolecular bonds that occur when a surface is created). But in ductile materials, plastic dissipation also contributes to G.

As mentioned, LEFM applies when the nonlinear deformation of the material is confined to a small region near the crack tip and plasticity does not play an important role during fracture. For brittle materials like some high strength steel, glass, and concrete, it accurately establishes the criteria for failure. However, severe limitations arise when the region of the material subject to plastic deformation before a crack propagates is not negligible. Additionally, LEFM has proven a useful tool for solving fracture problems provided a crack, like notch or flaw, exists in the structure.

In reality, the crack tip is surrounded by the fracture process zone, the region around the crack tip where nonlinear deformation and material damage occur. Inside this zone, the LEFM solution is not valid. Outside this zone, the LEFM is accurate provided the plastic damage zone is small enough. The objective of LEFM is to predict the critical loads that will cause a crack to grow in a brittle material. This is not always the case and for ductile metals the size of the nonlinear zone, due to plasticity or microcracking, is not negligible in comparison with other dimensions of the cracked geometry.

Moreover, even for brittle materials, where the process zone is small, the presence of an initial crack is needed for LEFM to be applicable. This means that bodies with no initial cracks cannot be analysed using LEFM. The facts mentioned above became the main motivation for development of a new field in fracture mechanics taking into account the plasticity in the process zone named EPFM.

1-2-2. Elastic-Plastic Fracture Mechanics

To predict failure in ductile materials, for which the assumptions of LEFM is no longer valid, EPFM provided the solution. Nonlinear fracture mechanics attempts to extend LEFM to consider inelastic effects. The theory is called Elastic-Plastic Fracture Mechanics; however, the theory is not based on an elastic-plastic material model, but rather a nonlinear elastic material. It is based on a nonlinear elastic power law material (the same as elastic-plastic material but different unloading path). Under monotonic loading, this nonlinear elastic material can be matched to the behavior of an elastic-plastic material whose hardening behavior is accurately modeled by a power law.

Rice (1968) made a considerable advance in EPFM. He idealized plastic deformation as a nonlinear elastic phenomenon for mathematical purposes and was able to generalize the energy release rate for such materials. He expressed this in terms of a path independent contour integral called J-Integral which became a very efficient tool to treat energy problems in fracture mechanics.

As mentioned earlier, LEFM is valid for materials for which the plastic zone around crack tip is small compared to the dimensions of structure or specimen (i.e. brittle materials). The J-integral represents a way to describe the case where there is suffcient crack tip deformation that the part no longer obeys the linear elastic approximation. This analysis is limited to situations where plastic deformation at crack tip does not extend to the furthest edge of the loaded part. It was shown by Rice that the J-integral is equal to the strain energy release rate for a crack in a body subjected to monotonic loading $(J = G)$. This is true both for linear elastic and non-linear elastic materials.

In this method, the elastic-plastic failure parameter is designated J_{Ic}. The stress intensity factor, K_{Ic}, can be calculated from the J-integral using Eq. 1-3. This relation has become a common technique to calculate stress intensity factors in both LEFM and EPFM for growing cracks.

In EPFM, a pre-existing crack is also assumed. No damage evolution is modeled and conventional material models, e.g. elastic-plastic constitutive equations, are applied. The process zone is assumed as infinitesimally small and special fracture criteria (e.g. K-based criterion or J-based criterion) for crack extension are required. EPFM covers a comparably small part of these constitutive theories and phenomena of inelastic deformation; and does not account for effects of load history, unloading, and local rearrangement of stresses.

Methods of conventional fracture mechanics are successfully used for the assessment of engineering structures for a very long time. In many cases, LEFM or EPFM is still applied to predict fracture onset due to its high level of standardisation and experience. However, considering the LEFM and EPFM limitations, failure prediction in a more general case requires modelling of the failure process zone.

An alternative approach to predict fracture, which overcomes some of the aforementioned difficulties, is local approaches and micromechanical modeling of damage and fracture. As in Siegmund et al. (2000) pointed out, to date, local approaches are the only really successful methods for prediction of crack growth resistance.

In a local approach, in principle, the parameters of the model depend only on the material, and not on the geometry. In this kind of approach, one can simulate ductile fracture either by employing a micromechanical model of damage, which represents the micromechanics of void initiation, growth and coalescence or by using a phenomenological model (like CZM) for material separation and coupling the model to the surrounding undamaged elastic–plastic material.

1-3. Literature Review

Fracture can be analyzed experimentally, analytically, or numerically. Experimental analysis can be extremely costly and time consuming. The other alternative to predict structural resistance capacity is simplified analytical methods like LEFM and EPFM. The overview of the application of analytical analyses and their main drawbacks has been described above.

Analytical and macroscopic fracture mechanics approaches have some limitations with respect to the amount of plasticity allowed at the crack tip, constraint and geometry dependency. LEFM and EPFM are constraint and geometry dependent, because they are applicable to structures with initial crack, and the structure without an initial flaw cannot be investigated by these methods. As no analytical solutions are possible in more general cases, and with advances in computer technology, the numerical methods and finite element methods (FEM) have become capable tools to assess structural integrity.

Although the FEM represents the most advanced approach, problems related to the prediction of fracture still need to be resolved. Fracture parameters and criteria for fracture and crack growth, which are used in practice for engineering assessment methods, have not yet been properly investigated. Presently, there is no adequate method to determine both fracture initiation and propagation in large scale structures. It is generally agreed that the models of the ductile fracture initiation and fracture propagation have not yet matured to a level of high general accuracy.

Numerical analyses of fracture can be done by one of the following approaches:

- Application of local fracture criteria
- Application of Cohesive Zone Model

Both approaches allow for splitting the total dissipated work in formation of the ductile crack into the work of separation in the process zone and the plastic work in the embedding material and, thus, solve a classical problem of fracture mechanics (Siegmund et al. 2000). In numerical simulation of the fracture, the process zone ahead of the crack tip is modeled by either cohesive elements or continuum elements with incorporated fracture criteria, whereas the rest of the structure consists of continuum elements with classical elastic-plastic constitutive behavior.

1-3-1. Fracture Criteria

In order to predict the onset of fracture using FEM, several failure criteria and damage models are proposed and implemented in the literature. Comprehensive study on the existing fracture criteria and damage models in various stress and strain states is presented by Tornqvist (2003). Tornqvist (2003) defines separate damage categories including:

- void growth fracture criteria,
- continuum damage models,
- porosity based models,
- and empirical criteria.

In the following, some of the criteria and the models will be discussed briefly to give an overview of this wide field of research.

There are numerous empirical fracture criteria. Most of them are simple criteria based on critical stresses or strains. The most simple and common one in Finite Element (FE) simulations is the equivalent plastic strain criterion. However, since the strain at fracture depends on the stress state and thus often varies for each situation, this criterion is an over-simplified fracture criterion. The governing damage processes in materials are highly influenced by the stress triaxiality, which should somehow be accounted for in the constitutive material model or in the damage criterion (Tornqvist, 2003).

Fracture in ductile materials relates to the formation, growth and coalescence of voids. Void growth criteria assume that the degree of void growth can be represented by a damage parameter. Once this parameter reaches a critical level, fracture is initiated. Continuum damage models couple the constitutive material laws to the damage evolution. The material may in this way experience a degradation effect (softening) during plastic deformation. Fracture occurs once the damage has reached a critical level.

Another damage category is the porosity based model. As for continuum damage models, the porosity models also couple damage to the constitutive material laws. The difference lies in the way the material damage is defined. Porosity based models couple damage directly to the physics of void growth. Continuum damage models, on the other hand, define damage as an evolution variable. The well-known porosity based damage model is the Gurson (1977) model. It was developed further by Tvergaard (1982) and Tvergaard and Needleman (1984) and called GTN model.

As seen, there are several possible models/criteria for analysing ductile fracture initiation in large structures. The advantage of this type of models is that it has a micromechanical basis and can be used to predict damage and failure of the material even in initially undamaged structures. The main drawback is that each damage criterion only covers a specific kind of failure mechanism and cannot be used anymore if another failure mechanism is activated.

Another problem with these damage models is that numerical simulations can show inherent mesh sensitivity. A fine mesh may for instance indicate strain concentrations at certain locations which may not be captured by a coarser mesh. The effect is especially apparent close to crack tips. When large elements are applied, the problem is that strain concentrations remain uncaptured. By increasing the element size, the stress and strain concentrations are reduced and this delays fracture.

In numerical analysis using the above mentioned fracture criteria, crack propagation is possible by using element deletion technique by which an element will be removed when it has reached the failure criterion value. This will often cause convergence problems as the stiffness is suddenly reduced or removed. This is an engineering approach which makes FE solutions very mesh sensitive and seems to be physically unreasonable.

Generally, crack growth can be numerically simulated in the following ways:

- Node release techniques, controlled by any fracture mechanics parameter (e.g. J-integral) which requires knowing the crack location in advance. This approach is mesh sensitive and the application of fracture mechanics parameters has some limitation as explained before.
- Element deletion based on fracture criteria which is mesh sensitive and cause numerical convergence problem.
- Material separation modeled by cohesive elements.

This study focused on the last approach and its application.

1-3-2. Cohesive Zone Modeling

A "phenomenological local approach" used for the numerical simulation of the crack initiation and propagation is known as the Cohesive Zone Model (CZM) (Siegmund et al., 2000). Cohesive elements used in simulating ductile fracture are supposed to represent the mechanism of nucleation, growth and coalescence of microscopic voids. CZM is based on an idea proposed by Dugdale (1960) and Barenblatt (1962).

Dugdale used this model to describe analytically the plastic deformation near the crack tip whereby the normal stress was limited by the yield stress of an elastic-ideally plastic material. Barenblatt investigated the fracture of brittle materials. Most of the recently developed and proposed models of CZM are different from Barenblatt's model in that they define the traction acting on the crack surface in dependence on the opening and not on the crack tip distance as Barenblatt did.

Although the concept of CZM originates back to the early sixties of the previous century, the concept has gained wide spread use only within the recent years. CZM application as a fracture model occurred substantially later, using the finite element analysis method. In a finite element representation of CZM, originally proposed by Hillerborg et al. (1976) for brittle fracture, cohesive elements are introduced as interface between continuum elements. CZM has also been applied to ductile damage starting with an investigation by Needleman (1987) for the microscopic modelling and by Tvergaard and Hutchinson (1992) for macroscopic failure.

Beside the simulation of failure in metals, the cohesive model has been widely used in the last three decades for fracture in fibers, polymers, and concrete structures. Most of the researchers investigate the application of CZM to simulate fracture in different kind of standard fracture specimens.

Cornec et al. (2003) developed experimental procedures which allow the determination of cohesive material parameters for the Traction-Separation Law (TSL). This method is also used in this thesis to predict the cohesive parameters.

Scheider et al. (2003) proposed a new cohesive law and used it for the prediction of the crack path during stable crack extension in ductile materials. Crack propagation was simulated in a round tensile bar. It was shown that the model is able to predict the failure mechanism, which consists of normal fracture in the center and combined normal/shear fracture at the specimen's circumference. The cohesive parameters can be different in normal and tangential direction, but several authors define the separation parameters to be equal for both failure modes. In Scheider et al. (2003) paper the parameters for normal and tangential fracture are completely independent.

Fracture in a notched round tensile bar is also modeled by Anvari et al. (2007) using CZM. The cohesive elements obey the TSL defined from the single element calculations. A single strain rate dependent element that obeys Gurson-Tvergaard-Needleman (GTN) formulation was examined under different values of stress triaxiality and loading rates. The resulting stress-elongation curves represented the TSL for cohesive elements.

In order to determine the TSL on a micromechanical basis, the deformation behaviour of a representative volume element, i.e. a single voided unit cell, including its material softening behaviour has been investigated in the literature. The first researchers who used this approach for the derivation of model parameters for cohesive modelling, were Tvergaard and Hutchinson (1992), who used a Gurson type model for the unit cell. However, they only studied a single stress state (uniaxial straining), and did not point out an issue, which becomes obvious by microstructural considerations: i.e. the TSL may depend on the stress state, which can be characterised by the triaxiality, $\eta = \frac{\sigma_H}{\sigma_{eq}}$, that is the hydrostatic stress divided by the Von Mises equivalent stress.

This issue was first investigated by Siegmund and Brocks (2000). The approach was extended to impact problems by using rate-sensitive and triaxiality-dependent cohesive elements to simulate crack growth under quasi-static and dynamic loading conditions by Anvari et al.(2006). In these studies, the constraint dependence of the cohesive parameters was considered by loading the representative volume element under different constraint conditions.

The approach already described is to transfer the deformation behaviour of the representative volume element, i.e. a single voided unit cell, to the cohesive elements. Scheider (2009) discussed that the main drawback of this method is that the unit cell contains both, deformation and damage of a material whereas the cohesive model should contain the material separation only. He presented a new approach, in which the behaviour of a unit cell is separated to elastic-plastic deformation and damage, and only the damage contribution is applied as the TSL for the cohesive elements.

It should be noted that the validity of the GTN model is limited with respect to the failure mechanism and also with respect to stress triaxiality. This makes the proposed identification procedure only applicable for a specific range of structures, unless a more sophisticated void growth model is utilised.

In the cohesive zone framework, the stress-state dependence of the fracture process under plane strain has been the subject of investigations during the last decade. Using void growth models on unit cells, triaxiality dependent TSLs have been developed and applied to various geometries (e.g. Anvari et al., 2006; Scheider, 2009; Siegmund et al., 2000). However, these analyses are difficult to perform using void growth models as they have difficulties in dealing with low triaxiality of thin-walled structures. So, in the case of the steel plate, the derivation of the parameter dependency on triaxiality based on void growth models cannot be applied.

An alternative to stress-state dependent CZM was presented in Scheider et al. (2006). The parameters for a specific range of triaxiality can be identified, and then the CZM can be applied with constant parameters to structures with similar constraint. The advantage of this method is that no explicit triaxiality dependence is needed (which is a problem for commercial finite element codes), and only tests for parameter identification in the triaxiality regime of the structure to be analysed have to be performed.

CZM application for low triaxiality (plane stress) was investigated by Scheider et al. (2011). It was shown that the global behaviour can be predicted with constant cohesive parameters for many real materials as long as only flawed structures are simulated, even though the local behaviour, e.g. the crack front shape, may differ. However, if initially uncracked structures are investigated, the consideration of triaxiality for the cohesive parameters is crucial.

In this thesis, the cohesive model will be described thoroughly as a model which has many advantages; and it will be used to simulate the crack initiation and propagation in steel plates.

Chapter 2: Cohesive Zone Modeling

2-1. Introduction

It was discussed that if the process zone is sufficiently small compared to structural dimension, classical fracture mechanics can be applied. If not, process zone and the forces that exist in the fracture zone must be taken into account. The most powerful way to model process zone is to use CZM. The general advantage, compared with classical fracture mechanics, is that, in principle, the parameters of the respective models are only material and not geometry dependent. Thus, these concepts guarantee transferability from specimens to structures over a wide range of sizes and geometries. It is not even necessary to consider specimens with an initial crack as also initially uncracked structures will break if the local degradation of material has exceeded some critical states.

In cohesive crack model, the process zone is modeled as an extension of the crack length up to a point called fictitious crack tip (Figure 2-1). In this region, a specific constitutive law is considered. According to this specific law, stress decreases with increase in crack opening according to a specific function. The real crack tip (or physical crack tip) is the point on the crack surface on which there is no stress (i.e. the normal opening is bigger than the critical opening).

CZMs are able to describe materials that exhibit strain-softening type behaviour. The basic assumption underlying them is the formation of a fictitious crack, as an extension of the real crack, referred to also as the process zone, where the material is still able to transfer stresses, although it is damaged,. The crack is assumed to propagate when the stress at the crack tip reaches the cohesive strength. When the crack opens, the stress is not assumed to fall to zero at once but to decrease gently with increasing crack width until a critical displacement is reached and the interaction vanishes.

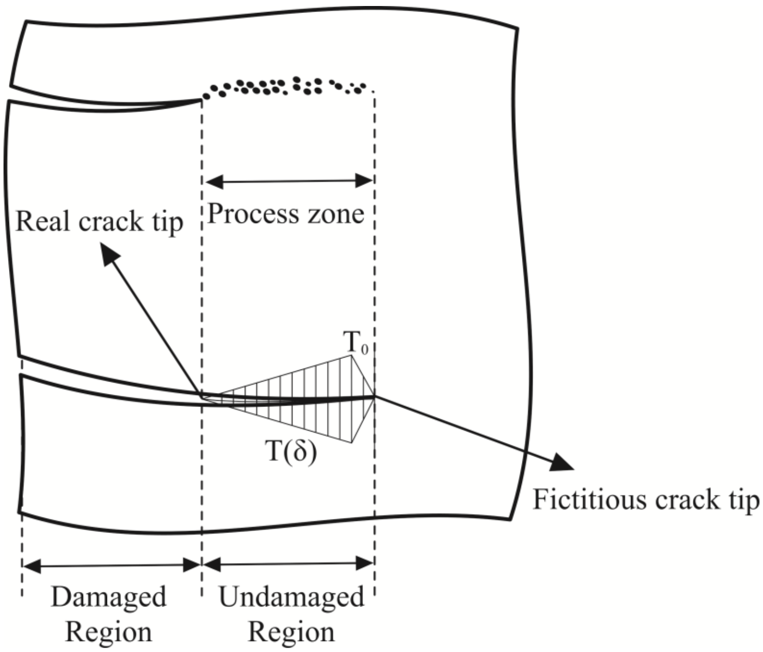

Figure 2-1: Process zone in cohesive crack model (Base on Carpinteri et al., 2003)

Within the framework of cohesive modelling and finite elements, contrary to computational crack propagation analyses using fracture criteria explained in the previous chapter, no continuum elements are damaged in the cohesive model. The zone in which damage occurs is reduced to a layer with zero thickness. The cohesive elements, in this layer, model the material separation; the surrounding continuum elements are damage-free. Cohesive interface elements are defined between the continuum elements, which open when damage occurs and lose their stiffness at failure so that the continuum elements are disconnected. For this reason the crack can propagate only along the element boundaries. If the crack propagation direction is not known in advance, the mesh generation has to make different crack paths possible.

The basic idea of the CZM, shown in Figure 2-2, is to split the material's behavior in deformation, which is modeled by continuum elements, and damage or separation, which is modeled by embedded interface elements within continuum elements. Ductile fracture process, consisting of initiation, growth, and coalescence of voids, is represented by a Traction–Separation Law (TSL), simulating the deformation and finally the separation of the material in the immediate vicinity of the crack tip. In the cohesive elements, the opening stress is controlled by a TSL, also called cohesive law. The separation, δ, can occur in normal (δ^N) or tangential direction (δ^T), which happen respectively in mode I and mode II/III fracture. Like the separations, the stresses, T, can also act in normal or in tangential direction, leading to normal or shear fracture respectively. Interface elements representing the damage are implemented between the continuum elements representing the elastic–plastic properties of the material.

In addition, by using CZM in FE analysis, mesh independency is expected as long as the cohesive elements adequately resolve the fracture process zone. This will be explained more in following parts.

The material separation and thus damage of the structure is classically described by interface elements, no continuum elements are damaged in CZM. Using this technique, the behavior of the material is split in two parts, the damage-free continuum with an arbitrary material law, and the cohesive interfaces between the continuum elements, which specify only the damage of the material (Figure 2-2). This modelling requires the use of a pair of constitutive equations: a stress–strain relationship for the undamaged material, and a stress-displacement curve for the damaged material.

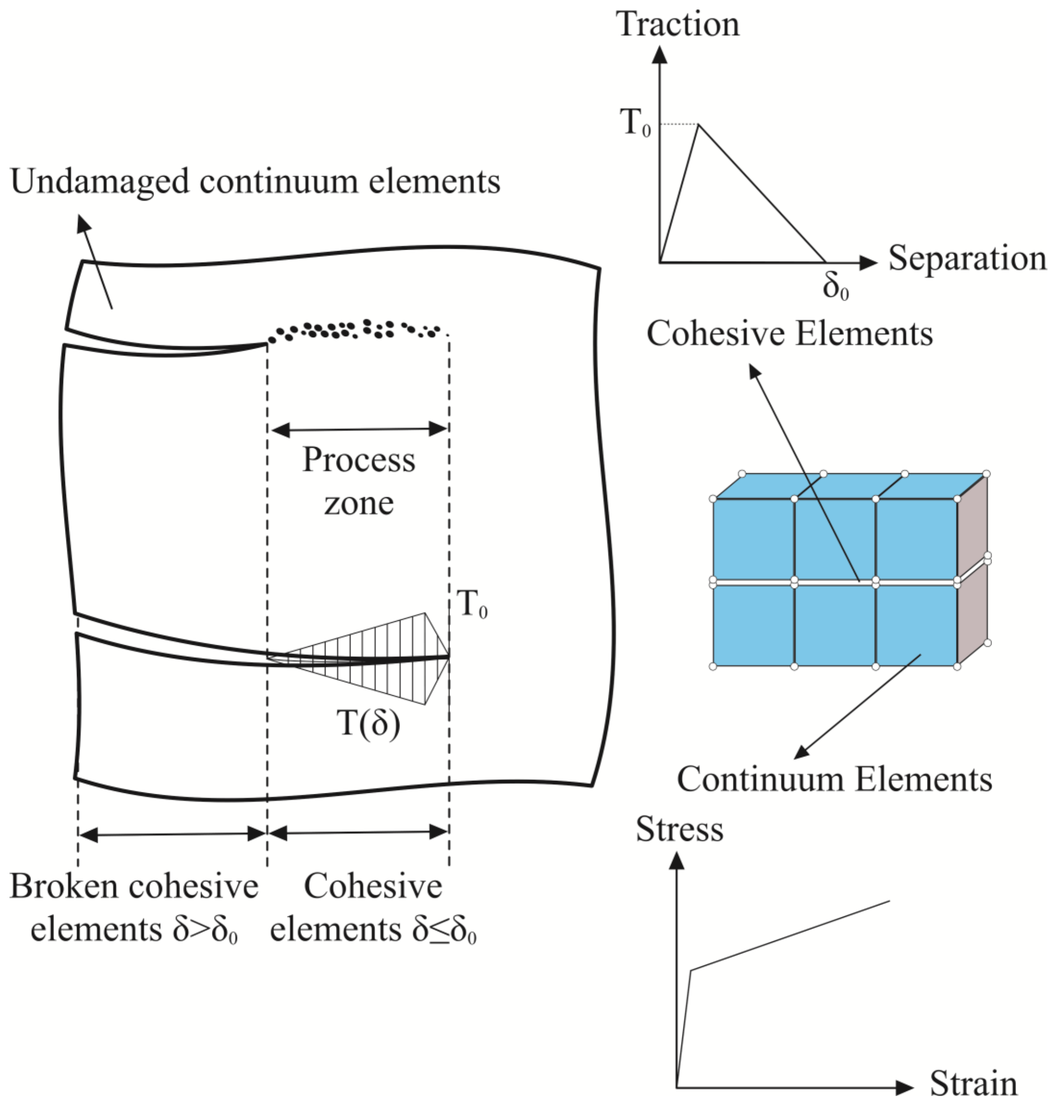

Figure 2-2: Basic concept of CZM and representation of the ductile fracture by CZM (Based on Cornec et al., 2003)

2-2. Cohesive Law

The cohesive constitutive model has two key parameters that characterize the decohesion process: The maximum traction (stress at the surface of the continuum element), T_0, also denoted as cohesive strength and the separation where the cohesive element fails, δ_0. When the normal or tangential component of the separation reaches a critical value, δ_0^N or δ_0^T , respectively, the continuum elements initially connected by this cohesive element are disconnected, which means that the material at this point has failed (Figure 2-3).

The separation of the cohesive interfaces is calculated from the displacement jump *[u]* between the adjacent continuum elements:

$$\delta = [u] = u^{+} - u^{-} \qquad \text{Eq. (2-1)}$$

u^{+} and u^{-} are the displacement of the upper node and the lower node respectively.

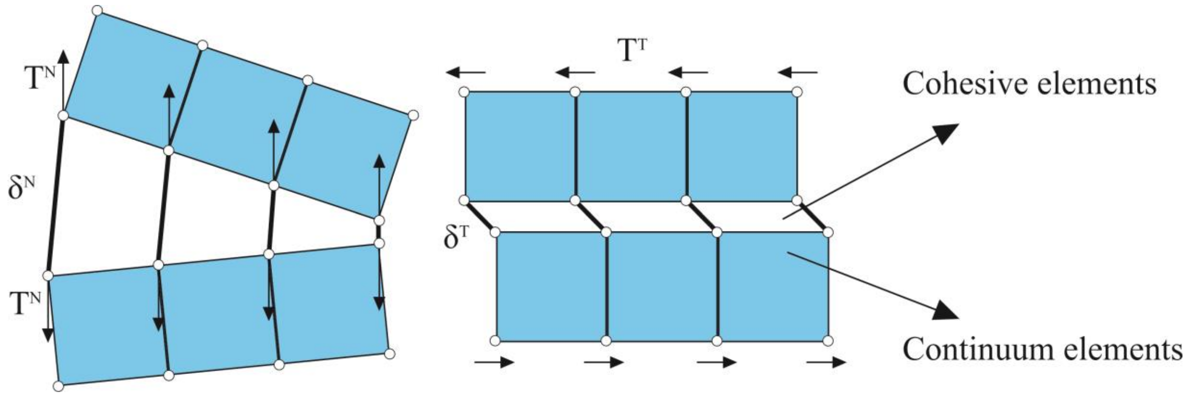

Figure 2-3: Representation of the activated cohesive elements (Based on Cornec et al., 2003)

A constitutive equation is used to relate the traction, *T*, to the relative displacement, *δ*, at the interface. The form of the cohesive law is given by the function *T(δ)*. The peak stress sets the local strength of the material and plays a critical role in developing plastic deformation in the background material. The area under the TSL curve is the energy absorbed by the cohesive element, Γ_0, and is known as the cohesive energy. This parameter, the total energy dissipation at fracture, Γ_0, can be derived by:

$$\Gamma_0 = \int_0^{\delta_0} T(\delta)\, d\delta \qquad \text{Eq. (2-2)}$$

If the shape of the TSL is known or presumed, two of the aforementioned parameters are enough to define the cohesive law.

The local work of separation is equal to the material toughness which equals the energy release rate, G_c, when the material follows a linear-elastic response. The value of Γ_0 can be obtained by experiment, since it coincides reasonably well with the J-integral at crack initiation, J_i. When the material deforms plastically, G_c elevates above Γ_0, but still the cohesive energy, Γ_0, corresponds approximately to the J-integral at crack initiation, and J_i can be the first guess for Γ_0.

The cohesive parameters can be different in normal and tangential direction, but several authors define the separation energy to be equal for both failure modes, i.e. $\Gamma_0^N = \Gamma_0^T$. It should be noted that not enough study has been performed for tangential separation in the literature.

The need for an appropriate constitutive equation in the formulation of the cohesive element is fundamental for an accurate simulation of fracture process. The shape of the CZM and its input parameters are often chosen as simple as possible for numerical reasons, rather than being physical meaningful. This is because the mechanisms that control those parameters have not yet been properly quantified. Since the cohesive model is a phenomenological model there is no evidence which form to take for $T(\delta)$. Basically, the TSL is assumed to be a stress–separation curve with a bilinear shape. More recently, different shapes of the CZM have been proposed, namely the trapezoidal shape and exponential forms. Most authors take their own formulation for the dependence of the traction on the separation. Some softening models that have been proposed are shown in Figure 2-4.

For ductile materials, a polynomial function of third degree, first used by Needleman (1987) for the pure normal separation and some years later extended by Tvergaard (1990) for mixed mode loading, is one of the most popular cohesive laws and used by many authors. Needleman (1990) also used the exponential curve form. The polynomial function was extended and implemented later by Scheider (2003). The cohesive law presented in Scheider (2003) is capable of shear separation and unloading. It is similar to the function presented by Tvergaard and Hutchinson (1992), as shown in Figure 2-4 and called trapezoidal form in the following.

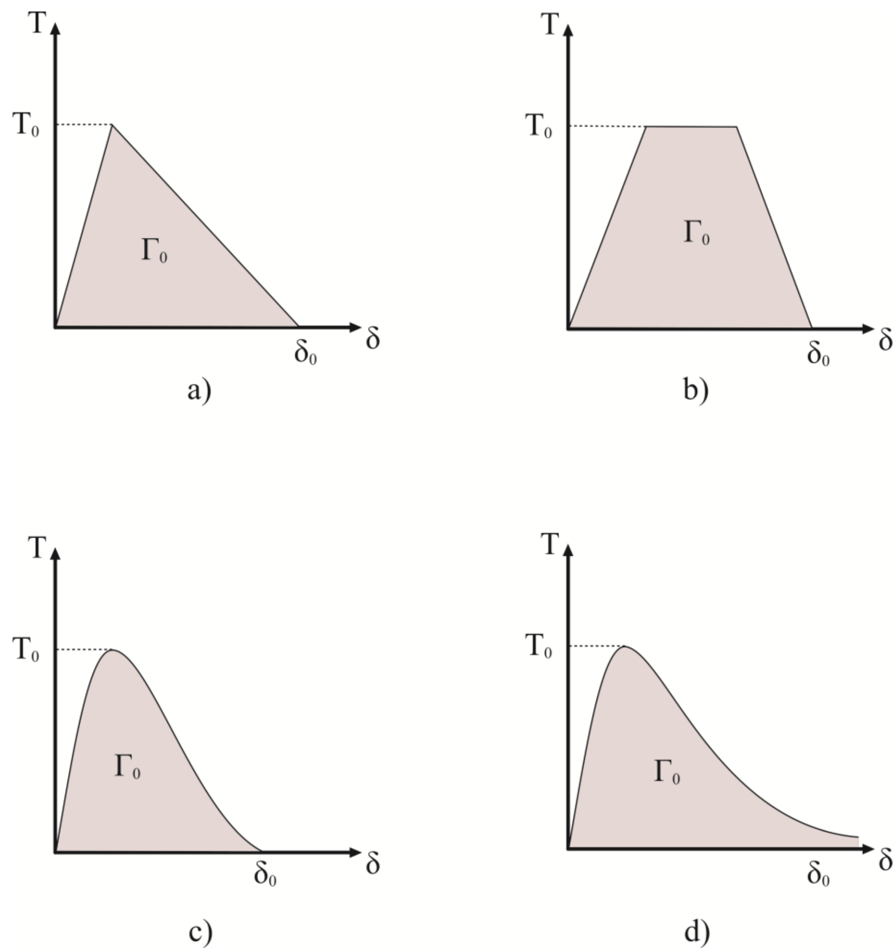

Figure 2-4: Form of the TSL a) bilinear, b) trapezoidal, c) cubic, d) exponential

One characteristic of all softening models is that the cohesive zone can still transfer load after the onset of damage. After the interfacial normal or shear tractions attain their respective cohesive strengths, the stiffness is gradually reduced to zero. They contain the two material parameters T_0

and δ_0 mentioned above; and for total failure, the stresses become zero, $T(\delta > \delta_0) = 0$ for both normal and tangential separation.

In traction-separation law, the initial slope is needed to avoid numerical problems between the cohesive elements and the surrounding continuum elements, and the descending slope models the rapid softening during void growth and coalescence.

Elices et al. (2002) stated that the form of the cohesive law depends on the class of material under consideration. The authors also stated that the cohesive law should not have a strain hardening part as only the continuum elements and not the cohesive elements are supposed to affect the global behavior of the structure. Additionally, the initial stiffness of the cohesive model should be chosen as high as (numerically) possible. It should be at least greater than the elastic stiffness of the adjacent continuum element, as the deformation of the structure has to be dominated by the deformation of the continuum elements.

The influence of the shape of the cohesive law on the crack propagation has not yet been studied extensively. Some investigations deal with the effect of the shape of the traction–separation function on the resulting fracture behaviour (e.g. Tvergaard et al., 1992; Scheider, 2009). Tvergaard and Hutchinson (1992) came to the conclusion that this effect can be relatively weak. It is often referenced to state that the shape of the cohesive law has little influence on the results. Although it has been claimed that the shape of the TSL hardly influences the crack growth behavior, there are a few investigations that show higher effects of the shape. For example, Scheider et al. (2006) showed numerically that the shape of the TSL can affect the load–displacement behavior. Scheider et al. (2006) tried to transfer constant cohesive parameters, which were derived for a specific TSL, to another TSL. It was shown that the cohesive elements are not transferable.

It seems that for each TSL a set of new cohesive parameters should be derived. The method that will be used in this research is to determine the cohesive parameters for a specific TSL by simulating tensile tests. Then, the same TSL with the same cohesive parameters will be used to predict fracture in the steel plates.

Another issue that should be considered while using CZM is the fact that if both separation modes, the tangential and the normal separation, occur simultaneously, there is an influence of the normal separation on the tangential tractions and vice versa. The description for this case of mixed mode and the basic assumptions made in the literature are given in the next part. Other special issues are the unloading behavior of the cohesive zone and the sliding of a failed cohesive element under negative normal separation, what involves contact of the fracture surfaces, described in the next part.

Initially, all cohesive models, in the literature, were only based on a pure mode I crack under monotonic loading. Improvements have been developed for the application to mixed mode loading, time dependence, interaction of combined normal and tangential loading, and unloading of the cohesive elements.

2-2-1. Mixed-Mode Fracture Criterion

Ductile fracture may occur in various modes:

- Normal fracture, where the fracture plane is perpendicular to the maximum normal stress (Mode I fracture).

- Shear fracture, where the fracture plane coincides with the plane of maximum shear stress (Mode II and III fracture).
- A combination of both which is typical for the fracture behaviour of thin sections; in this case, normal and shear modes are present.

As stated in the previous part, if normal separation, δ^N, and tangential separation, δ^T, occur simultaneously, there is an influence of the normal separation on the tangential tractions and vice versa. Under pure mode I, II or III loading, the onset of damage at the interface can be determined simply by comparing the tractions with their respective allowable values. However, under mixed-mode loading, damage onset may occur before any of the stress components involved reach their respective allowable values. Therefore, a general formulation for cohesive elements must deal with mixed-mode fracture problems.

The criteria used to predict crack propagation under mixed-mode loading conditions are generally established in terms of the energy release rates and fracture toughness. The most widely used criteria to predict the interaction of the energy release rates in mixed-mode is the power law given by the following expression:

$$(\frac{G_I}{G_{IC}})^\alpha + (\frac{G_{II}}{G_{IIC}})^\alpha + (\frac{G_{III}}{G_{IIIC}})^\alpha = 1 \quad \text{Eq. (2-3)}$$

The exponent α in the power law is usually selected to be either 1 or 2 in the literature. For isotropic materials $G_{IC} = G_{IIC} = G_{IIIC}$.

A recently proposed criterion, the BK criterion (Benzeggagh and Kenane, 1996), is established in terms of the single-mode fracture toughness G_{IC} and G_{IIC} and a parameter η for 2D fracture analysis:

$$G_{IC} + (G_{IIC} - G_{IC})\left(\frac{G_{II}}{G_T}\right)^{\eta} = G_{TC}$$ Eq. (2-4)

Where,

$$G_T = G_I + G_{II}$$ Eq. (2-5)

If mode III loading occurs the criterion is:

$$G_{IC} + (G_{IIC} - G_{IC})\left(\frac{G_{shear}}{G_T}\right)^{\eta} = G_{TC}$$ Eq. (2-6)

Where,

$$G_T = G_I + G_{shear}$$ Eq. (2-5)

$$G_{shear} = G_{II} + G_{III}$$ Eq. (2-6)

For isotropic material $G_{IC} = G_{IIC} = G_{IIIC}$, so the response is insensitive to the value of η. In many cases the one-dimensional representation of the relation is sufficient, namely when only mode I fracture is concerned.

Another proposed mixed-mode criterion assumes that damage initiation can be predicted using the quadratic failure criterion:

$$\sqrt{(\frac{< \sigma >}{T^N})^2 + (\frac{\tau_1}{T^T})^2 + (\frac{\tau_2}{T^T})^2} = 1$$ Eq. (2-7)

where σ is the normal traction, and τ_1 and τ_2 are the tangential tractions. T^N and T^T are the normal and shear cohesive strengths, respectively. The operator $< \sigma >$ is defined as x if $\sigma > 0$, and 0 otherwise.

The other way to embed the influence of tangential on normal opening (and vice versa) is to define the normal traction dependent on δ^T explicitly, as Scheider et al. (2003) assumed. In both cases the separation function does not only depend on δ^N, but also on δ^T. Generally, TSL can be written as:

$$T^N = T^N(\delta^N, \delta^T) \qquad \text{Eq. (2-8)}$$

$$T^T = T^T(\delta^T, \delta^N) \qquad \text{Eq. (2-9)}$$

2-2-2. Unloading in Cohesive Elements

Unloading in cohesive elements can occur in the cases of unloading of a structure or crack happening. Therefore, the behavior of the cohesive elements has to be defined under unloading which will lead to decreasing separation. The terms ‘‘loading’’ and ‘‘unloading’’ will be used when separation is increasing or decreasing, respectively, as the tractions decrease also under increasing separation beyond maximum stress, T_0, in the softening region of TSL. Unloading model should consider the irreversibility of the damage process. Since damage evolution is an inelastic deformation and nonlinear process, the separation in cohesive models are considered like plastic deformation.

In ductile materials, the mechanical work for producing damage is totally dissipated. Void growth in ductile materials is, hence, inelastic local separation and irreversible, and any unloading and reduction of separation occurs purely elastically with unchanged elastic stiffness as shown in Figure 2-5. If the local tractions in the cohesive elements are reduced to zero (AB in Figure 2-5), a significant separation remains. If the separation increases again, the tractions increase linearly up to point A and then follow the original cohesive law again. In the current implementation of the cohesive model, the slope of the unloading curve is also set equal to the initial stiffness of the cohesive law.

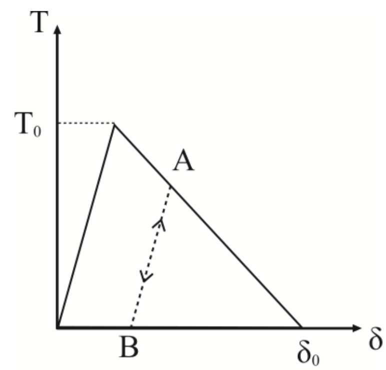

Figure 2-5: TSL at unloading

The contact condition, i.e. prevention of penetration of adjacent continuum elements during unloading, has to be ensured also after total failure of the cohesive elements. For mode I fracture, which is considered solely throughout this research, the contact reduces to a normal contact. However, if a structure fails under shear mode loading, frictional sliding of the fracture surfaces must be also taken into account.

2-3. Cohesive Parameters Determination

In this part, the identification and validation of the cohesive model parameters are explained. A general concept for their identification in the case of mode I fracture is explained.

Mixed-mode fracture is a relevant failure mechanism happens in homogeneous thin plates. The crack initiates in the centre of the specimen in normal fracture mode and then, continues to the surface of the plates in approximately 45 degree, which is called slant fracture. The mode I separation in this study represents the actual slant failure, and the respective cohesive parameters, T_0^N and δ_0^N, are hence effective values of a mixed mode situation. Therefore, here, only mode I fracture, which represents the real slant fracture, is considered for the fracture analysis.

The cohesive model, which describes the material damage in the process zone, is purely phenomenological. Because, in reality, damage does not happen only within a specific layer of cohesive elements, but volumetric elements are damaged. Although the cohesive parameters are phenomenological, they have a physical background. In the following, an engineering approach for the determination of the cohesive parameters for normal fracture in ductile materials will be presented which was proposed and applied by several researchers including Cornec et al. (2003).

The cohesive strength, T_0, can be taken as the maximum stress at fracture in a tensile bar. It has to be noted that the tensile specimen does not fail in a pure mode I. In slant fracture, a shear mode contribution is also present. As mentioned earlier, in this study, mode I cohesive parameters represent the parameters of mixed mode fracture.

Given the small plastic zone size, any elevation of G_c over Γ_0 is neglected and it is assumed that $\Gamma_0 = G_c = J_i$. The cohesive energy for normal fracture, Γ_0, is equal to the J-integral at crack initiation in mode I, J_i. J_i is usually identical to the intersection point between a JR-curve and the critical Stretch Zone Width (SZW_c), determined from the fracture surface. The principle of this method is shown in Figure 2-6 a.

JR-curve is a tearing resistance curve, represents a material resistance to progressive crack extension (this implies that a material's fracture toughness can change with crack extension). A tearing resistance curve is a plot of fracture toughness against crack extension. In many ductile materials, the size of the plastic zone at the crack tip increases as the crack extends. Thus, each successive unit of crack extension requires more energy than the preceding unit of extension (in order to further increase the plastic zone size). Hence, the resistance of the material to crack extension increases with crack extension. This type of behaviour is known as a rising R-curve. There is a limit to this increase in toughness, and hence, all R-curves eventually flatten off. JR-curve can be determined by a standard fracture test according to ASTM E1820.

The SZW_c should be determined by optical measurement of the stretch zone width of the initial fracture surface of the tested specimen. The intersection point of the average SZW_c and the J-Δa curve defines J_i. It is considered to be the most accurate method for measuring J close to the onset of crack extension.

As mentioned earlier, the determination of J_i require the use of optical measurement to measure the stretch zone width on the fracture surfaces of the specimens. The method can produce large scatter in the values of J_i as a result of the subjective interpretation and measurement of the stretch zone width. If the stretch zone width cannot be distinguished from ductile crack extension, J_i cannot be determined. Since there are practical difficulties in using this approach, which makes it unsuitable for routine materials testing, an alternative procedure for estimating J close to the onset of initiation of stable crack extension is proposed in Schwalbe et al. (1995). This approach is used in this thesis to determine the fracture energy.

The engineering approach is to use the fracture parameters at 0.2 mm of the crack extension. $J_{0.2}$ is the material resistance at 0.2 mm of the total crack extension. For many materials, this parameter provides useful estimation of the initiation toughness. This method is illustrated in Figure 2-6 b.

As in this study, no JR-curve, which is determined through the mechanical test according to ASTM E1820, are available, an alternative procedure is applied. JR-curve for small crack extension is taken from the blunting line (proposed by Cornec et al., 2003), which is given by a validated analytical solution:

$$J = 3.75\sigma_U . \Delta a \quad \text{Eq. (2-10)}$$

Where, σ_U is the maximum tensile strength and Δa is the crack extension. In this case, no determination of the J-integral by conducting standard fracture tests is needed. This method is presented in Figure 2-6 b.

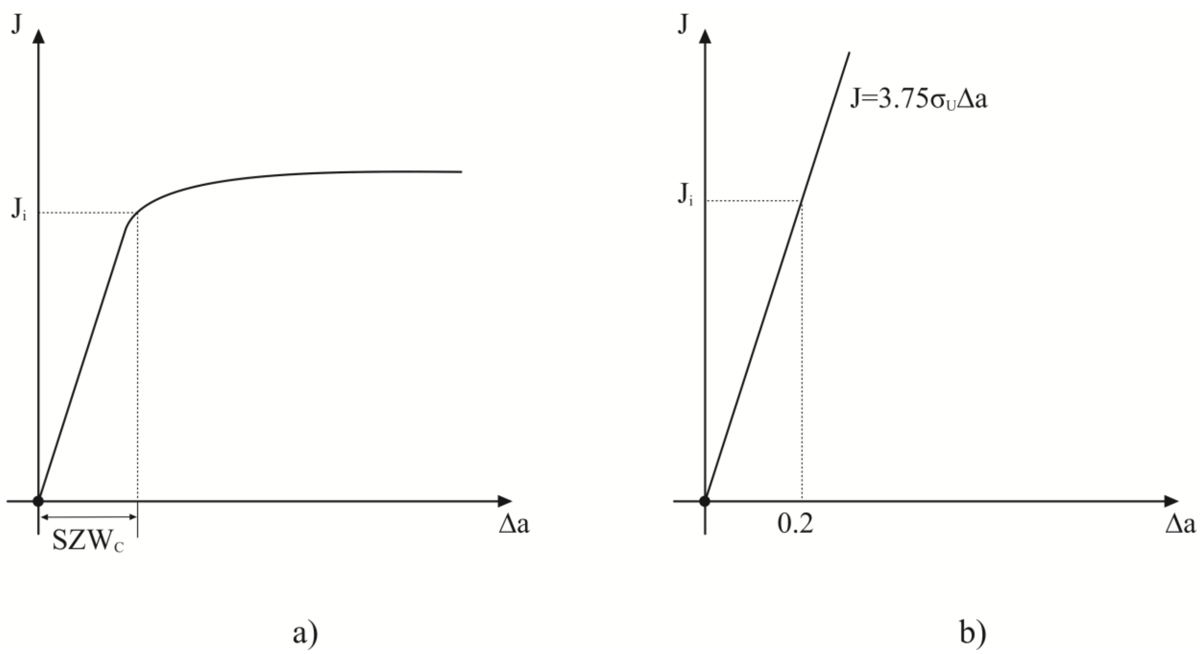

Figure 2-6: Determination of the cohesive energy by using a) the resistance curve and the stretch zone width, b) the analytical blunting line and 0.2 mm crack extension

The procedure described in this part will be used in Chapter 4 to determine cohesive parameters, T_0 and Γ_0 for a bilinear TSL. Cohesive parameters are calibrated by tensile tests and then, the same parameters will be applied for simulating the fracture in steel plates.

Chapter 3: Experimental Results

3-1. Introduction

In order to validate the fracture process that will be modeled by CZM in this thesis, experimental results are needed. The mentioned experiments were designed and performed in a simultaneous project (Jamaly, 2014) at Memorial University of Newfoundland to examine fracture process in steel plates experimentally. An overview of the experiments, test setup, and the results are mentioned in this chapter. These experimental results will be compared with numerical results, which will be modeled by CZM in Chapter 4.

Several fracture tests were conducted on two different kinds of steel materials. One is mild steel with 3.175 mm thickness, and the other is high tensile steel with 6.35 mm thickness. The mechanical properties of both kinds of steel materials are determined by conducting tensile tests and analyzing the experimental data. Then, fracture tests on steel plates, made from the same material as the tensile specimens, are investigated by conducting plate fracture tests.

3-2. Tensile Test

In order to determine material mechanical properties, mechanical tests are conducted where different parameters are measured. One of the useful and simple tests for determining the load-carrying capacity of the material is the tensile test of flat bars or rods, which relates stress and strain. According to ASTM E1820, flat tensile specimens are used for analyzing mechanical properties of plates.

In this tensile test, the specimen is subjected to a continuously increasing uniaxial load at constant rate (0.1 mm/sec) during which simultaneous measurements of the load and the extension are made. The force applied and the deformation that is produced can be used to calculate the stress and strain in the material.

From these measurements, the stress-strain curve is constructed. The stress (calculated from the load) and strain (calculated from the extension) can either be plotted as “nominal stress” against “nominal strain” or as “true stress” against “true strain”.

Engineering stress and strain are other expressions for the nominal curve indicated above. In this case, the stress is the ratio of the applied load to the original section area of the specimen. Assuming that the stress σ is distributed uniformly over the cross-section, we can write:

$$\sigma = \frac{P}{A} \qquad \text{Eq. 3-1}$$

The relation between the applied stress and strain, in elastic region, can be expressed by:

$$\sigma = Ee \qquad \text{Eq. 3-2}$$

Here *e* is the average linear strain. In simple terms, the linear strain can be expressed as:

$$e = \frac{l - l_0}{l_0} \qquad \text{Eq. 3-3}$$

l_0 is the gauge length of the specimen. Thus, *e* is the ratio of the change in the gauge length to the original gauge length. This strain is called the engineering strain and it is valid for small strain values. A different and useful concept for defining strain, when deformation is considered in more practical terms, is associated with the instantaneous change occurring in a specimen’s length while a force is acting on it. Unlike cases of engineering strain, where reference was made to the constant gauge length of the specimen, reference is made to changes in the dimension at each instant of the test. If dl is the amount by which the length, l, changes, strain can be defined similarly as:

$$\varepsilon = \frac{dl}{l} \qquad \text{Eq. 3-4}$$

Integrating the above equation:

$$\varepsilon = \int_{l_0}^{l_i} \frac{dl}{l} = ln\frac{l_i}{l_0} \qquad \text{Eq. 3-5}$$

ε is known as the natural, true, or logarithmic strain at every instant. It is often required to alternate between these two definitions of the strain, the engineering strain and the true strain. This can easily be performed using Eq. 3-3 and 3-4, as shown below.

$$\varepsilon = ln\frac{l}{l_0} = ln(e+1) \qquad \text{Eq. 3-6}$$

In plastic deformation, the volume remains constant, so:

$$V = A_0 l_0 = A_i l_i = \cdots = A_f l_f \qquad \text{Eq. 3-7}$$

A_0 and l_0, A_i and l_i, A_f and l_f are, respectively, the section area and the gauge length of the tensile specimen before the specimen extension, during the tensile test , and at the fracture.

There is a relation between true stress, σ_T, and engineering stress ,σ_E, using Eq. 3-6 and 3-7 as follows:

$$\sigma_T = \frac{P}{A_i}\frac{A_0}{A_0} = \frac{P}{A_0}\frac{A_0}{A_i} = \sigma_E\frac{A_0}{A_i} = \sigma_E\frac{l_i}{l_0} = \sigma_E(e+1) \qquad \text{Eq. 3-8}$$

The material properties of steel are determined by tensile tests on steel flat bars. The geometry of the tensile specimen is shown in Figure 3-1.

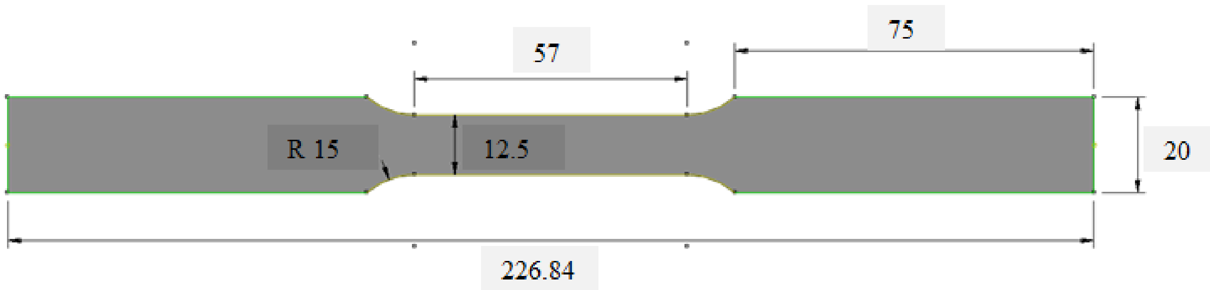

Figure 3-1: The dimensions of the tensile specimens (in mm)

Ten tensile specimens have been manufactured for the determination of the stress-strain curve of every kind of steel. The tensile specimens after the tensile tests are shown in Figures 3-2 and 3-3.

Figure 3-2: Steel tensile specimens after fracture - 3.175 mm thickness

Figure 3-3: Steel tensile specimens after fracture- 6.35 mm thickness

Experimental data and load-displacement curve obtained from the tensile tests, are presented in Figure 3-4 for thin specimens and in Figure 3-5 for thick ones. These curves are analyzed to derive engineering stress-strain curves using Eqs. 3-1 and 3-3. Engineering stress-strain curves are converted to true stress- strain curves by Eqs. 3-6 and 3-8. The stress- strain curves for one sample of the thin plate and one sample of the thick plate are demonstrated in Figures 3-6 and 3-7 respectively.

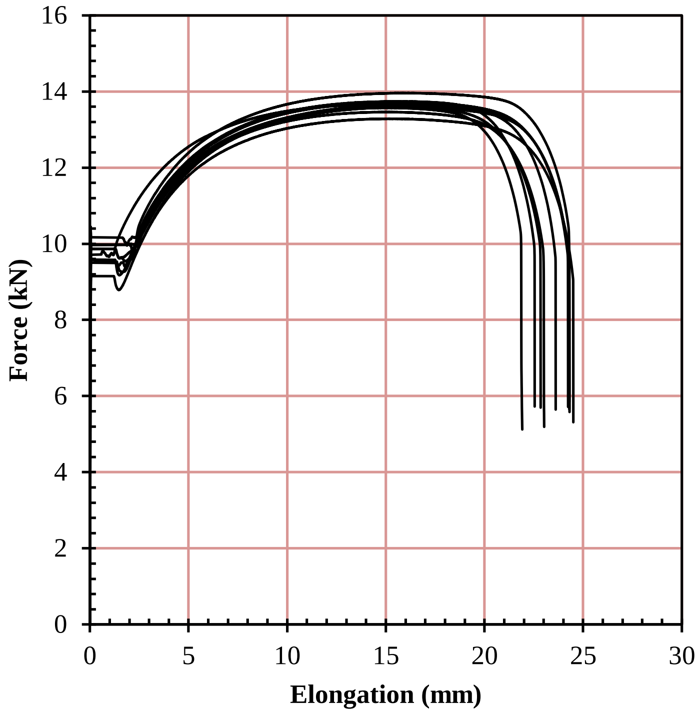

Figure 3-4: Force-elongation curves of steel tensile specimens- 3.175 mm thickness

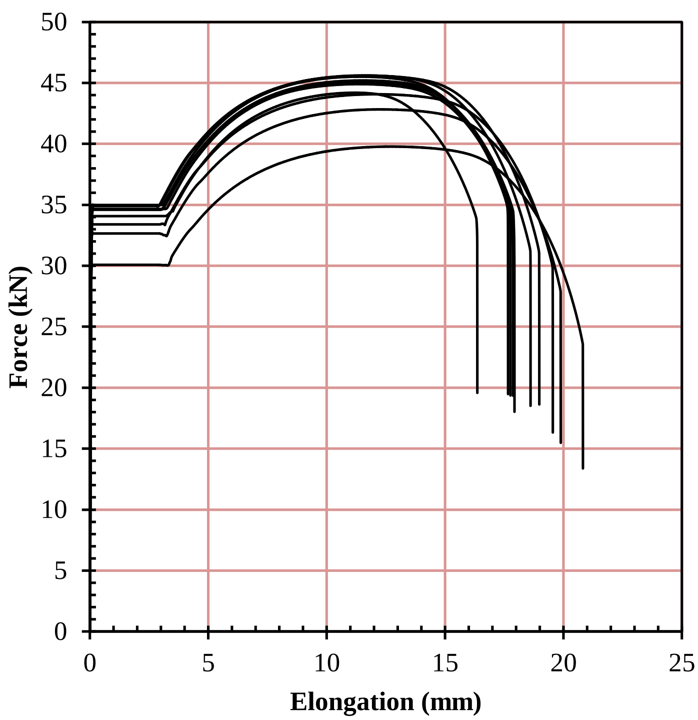

Figure 3-5: Force-elongation curves of steel tensile specimens- 6.35 mm thickness

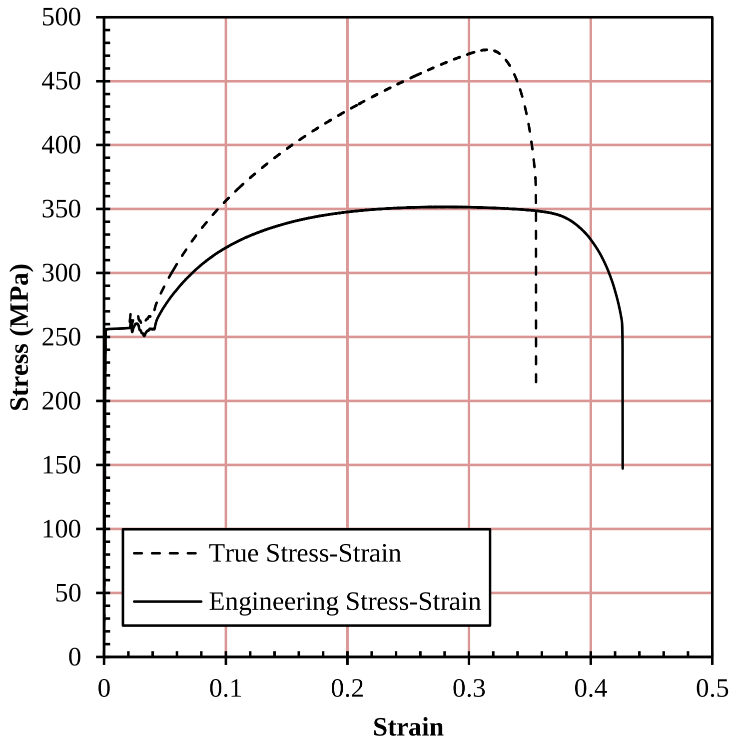

Figure 3-6: Engineering and true stress-strain curves- 3.175 mm thickness

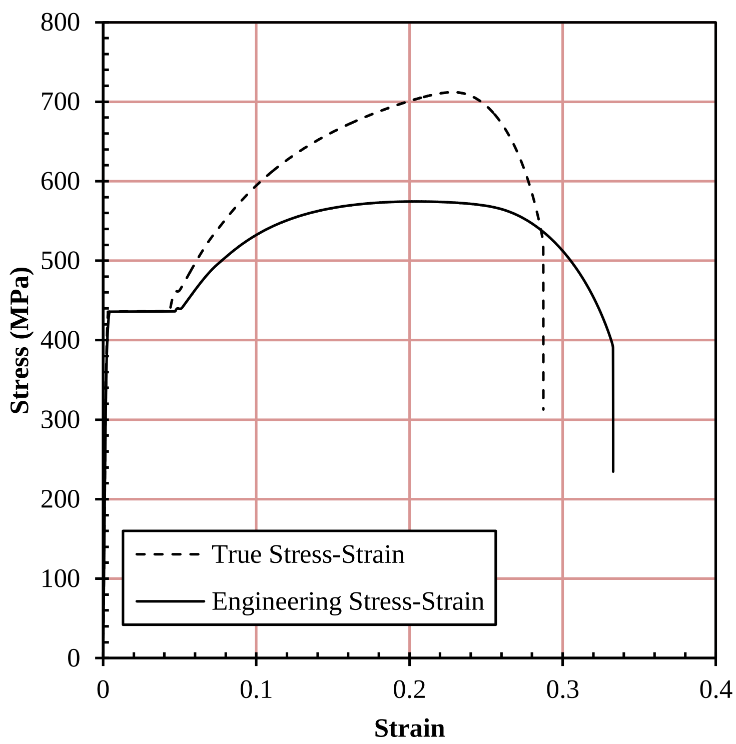

Figure 3-7: Engineering and true stress-strain curves- 6.35 mm thickness

In Figure 3-4 to Figure 3-7, the flat regions of the curves are the result of modifications on the experimental data. It should be noted that since the elastic region of the experimental curves deal with very small elongations/strains, the data obtained solely from the displacement sensor on INSTRON machine is not reliable and an extensometer must be used to measure, accurately, very small displacements in the tensile specimens. Measuring crosshead deflection during a test does not just measure strain in a defined region of a test sample. It also measures machine deflection, grip deflection, and possible slippage and deflection of the part of the test sample outside the normal reduced section. Hence, the change in length is not correctly measured due to the other deflections without an extensometer.

For the highest accuracy of the measurements of yield strength and Young's modulus, an extensometer is required to measure the change in length over the defined area. The extensometer and the way it is installed on the tensile specimen are shown in Figure 3-8.

The measuring range of the extensometer is very important. In general, the extensometer's measuring range should match the amount of specimen elongation that is being investigated. In the case of fracture analyses, the whole range of the elongation till the fracture is under investigation. To obtain the whole stress-strain curve, an extensometer with high measuring range is required. However, the available extensometer is applicable only for elastic region and insufficient measuring range of the extensometer prevents measurement of larger elongations.

One way to obtain data for the full stress-strain curve with a low measuring range extensometer is as follows: Run the test until a certain strain is reached, pause the test, remove the extensometer, and resume the test using the crosshead to obtain the rest of the test data to specimen failure. This procedure allows approximate measurement of elongation to failure with a low measuring range extensometer. Using this procedure will reduce the chance of damage to the extensometer. However, not all test controls allow you to pause the test. Finally, it is possible to use a long measuring range extensometer and get more accurate measurements.

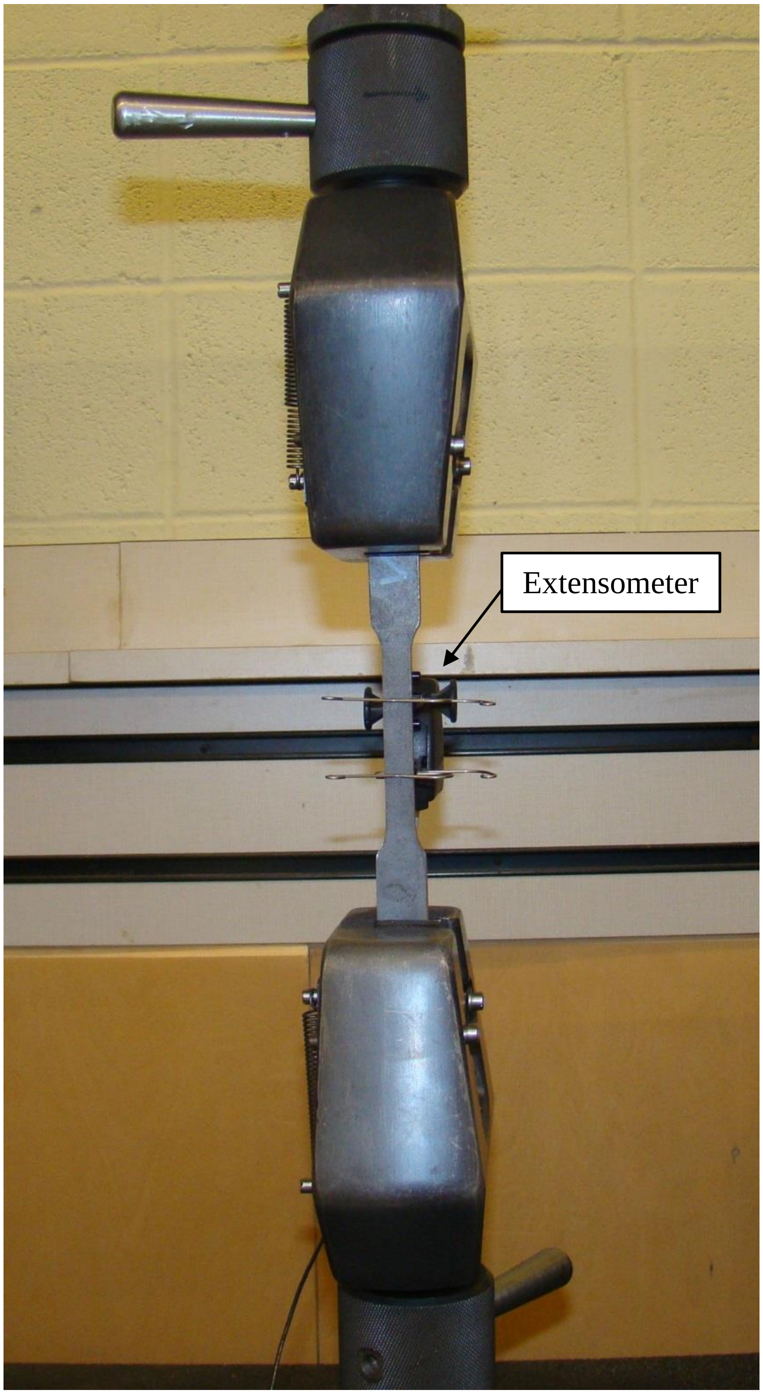

Figure 3-8: Tensile test setup, INSTRON machine, and extensometer

In this study, the elastic properties, ultimate stress, and the fracture point are essential which are measurable by presented curves in Figure 3-4 to 3-7. The horizontal flat regions in the mentioned curves are caused by simply connecting the elastic region measured by extensometer and the plastic area measured by sensors of the INSTRON machine.

The early stages of the tensile tests are used to evaluate the yield strength and the Young's modulus. The elastic limit is defined as the stress at which plastic deformation begins; in other words, it represents the largest load that a material can tolerate without noticeable or even measurable permanent change. Below this value, the slope, namely the ratio of stress to strain, is constant. The material is said to behave according to Hooke's law and the ratio of stress to strain is called young's modulus (E).

The need for a practical determination of yielding in a material resulted in a method for its evaluation, a technique known as the "offset yield strength". Offset yield strength represents the practical yield strength for engineering applications. For its evaluation, the early stages of tensile tests are used to evaluate the "yield strength", which is defined as the stress at which a predetermined amount of permanent deformation occurs. To find the yield strength, a predetermined amount of permanent strain is set along the strain axis. A straight line is drawn parallel to the linear portion of the stress-strain curve. The point of intersection of this line and the stress-strain curve is projected on the stress axis; this stress value is called the yield stress. The offset stress usually used for yield stress is at 0.002. This technique is illustrated in Figure 3-9.

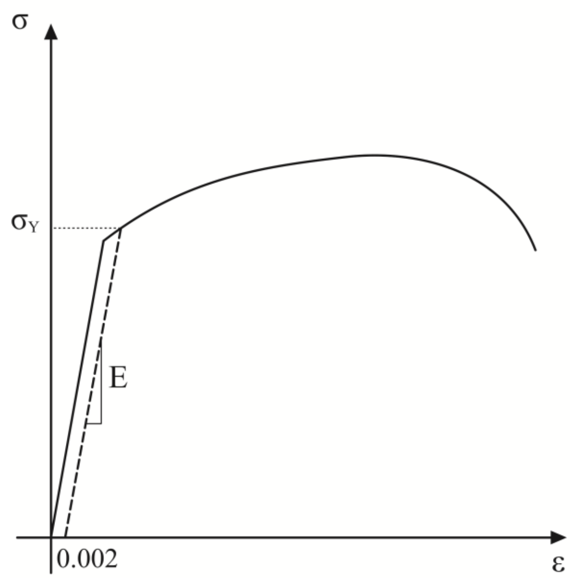

Figure 3-9: Determination of the elastic limit

Using the explained procedure for determining mechanical properties, the average material properties of steel are presented in Table 3-1.

Table 3-1: Mechanical properties of steel

Material	Young's Modulus (MPa)	Poisson Ratio	Yield Stress (MPa)
Mild steel	214000	0.3	244
High Tensile Steel	202000	0.3	426

3-3. Plate Fracture Test

In order to estimate the response of a steel plate to extreme loads, steel plates subject to indentation loads were tested in the Structural Laboratory at Memorial University of Newfoundland by Jamaly, 2014. The plate specimens were made of the same steel plates as the tensile specimens. A schematic view of the test setup is illustrated in Figure 3-10. Figure 3-11 shows the dimensions of the test setup.

Figure 3-10: Plate fracture test setup at the structural lab (Jamaly, 2014)

Two thin plates made of mild steel (3.175 mm thick) and two thick plates from high tensile steel (6.35 mm thick) were fabricated. The dimensions are shown in Figure 3-12. Since the main purpose of this study is to numerically simulate the normal fracture, and in order to avoid the fracture due to shear limit in the boundary of the plate, the two edges that the steel plate is placing on them are curved and the plate under investigation is designed to be wider at the edges. The width of the steel plates in the middle of the specimens is 100 mm.

The steel plate is bolted to the test setup to have approximately fixed boundary conditions at two edges of the plate. A semi- cylindrical rigid indenter is pushing the steel plate down until fracture happens. The impact speed is 0.1 mm/sec and the radius of the indenter is 75 mm. Broken steel plates are presented in Figure 3-13 and 3-14.

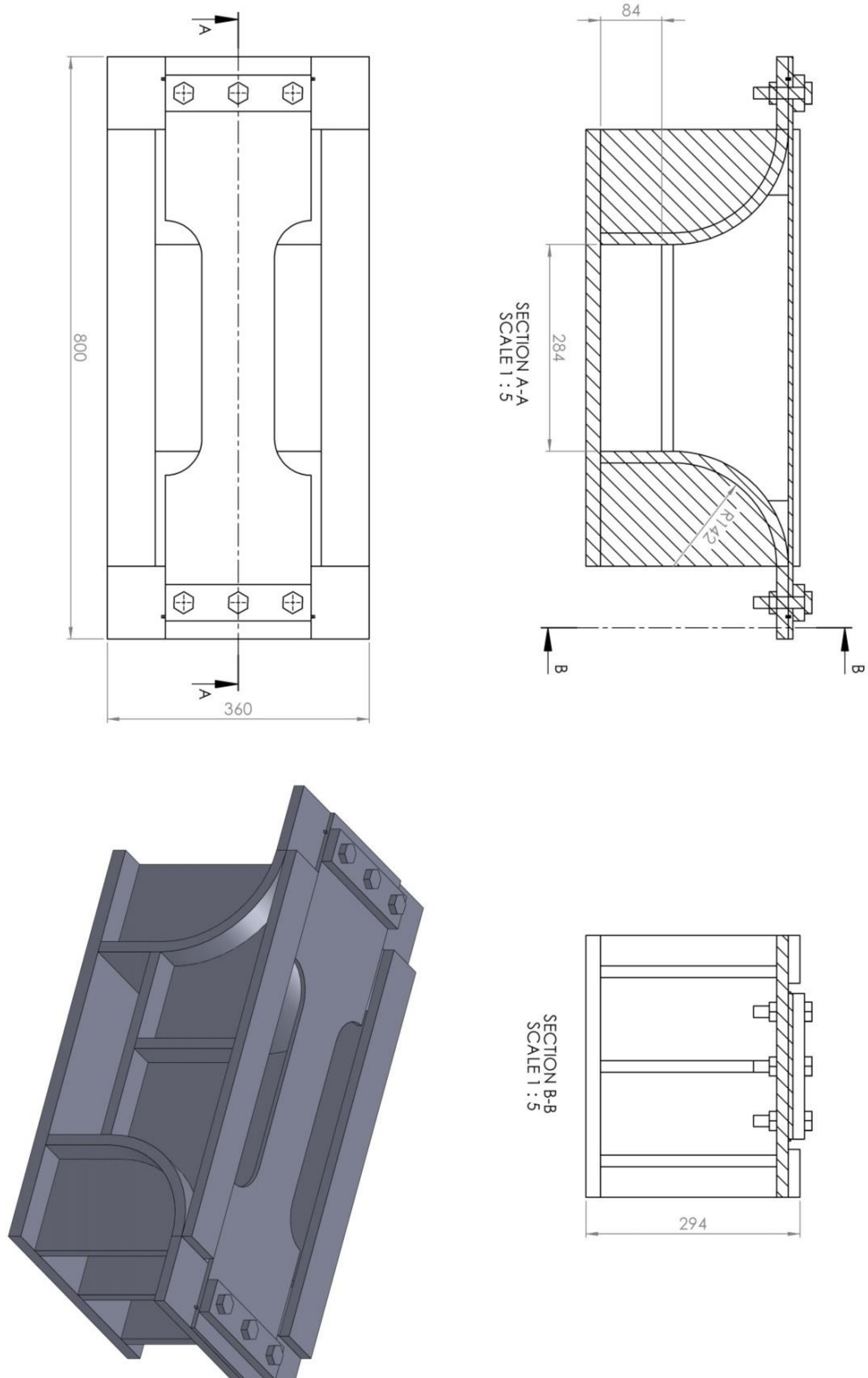

Figure 3-11: Dimensions of the plate fracture test setup (in mm) (Jamaly, 2014)

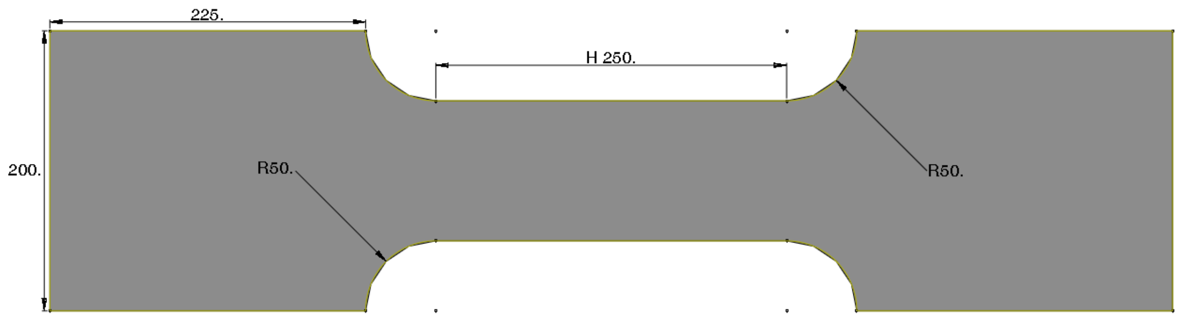

Figure 3-12: Steel plates dimensions (in mm)

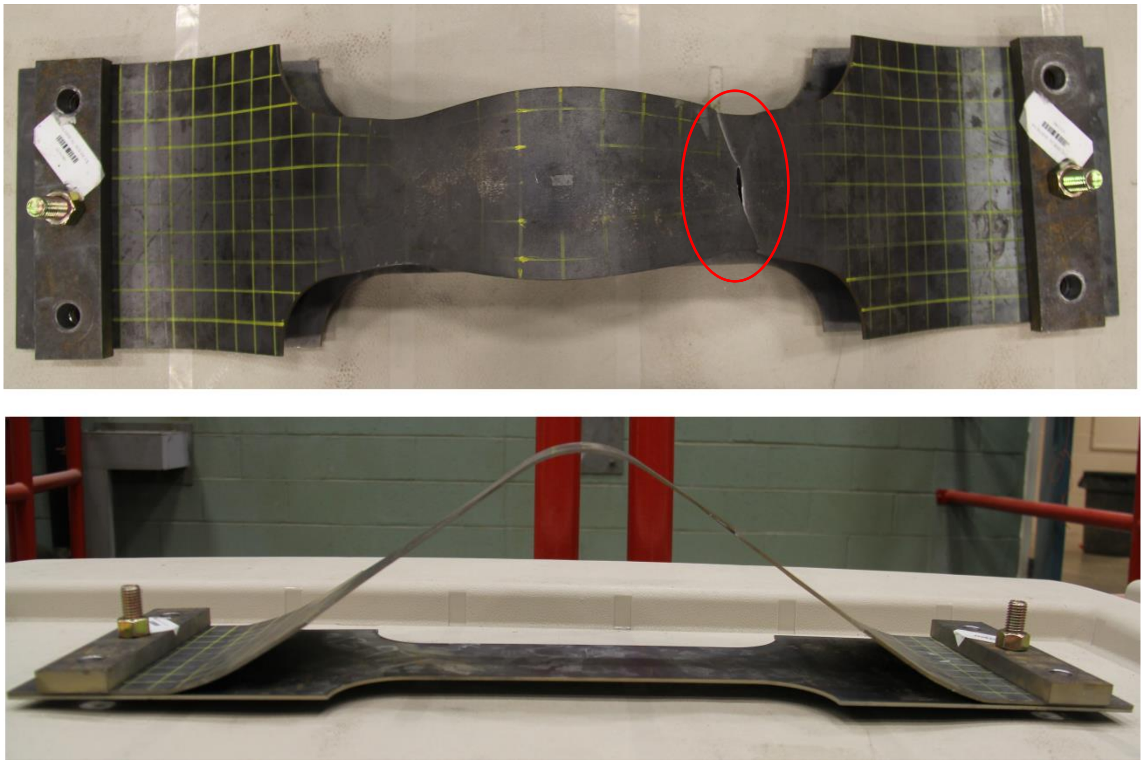

Figure 3-13: Crack path and the deflection in the thin plate (Jamaly, 2014)

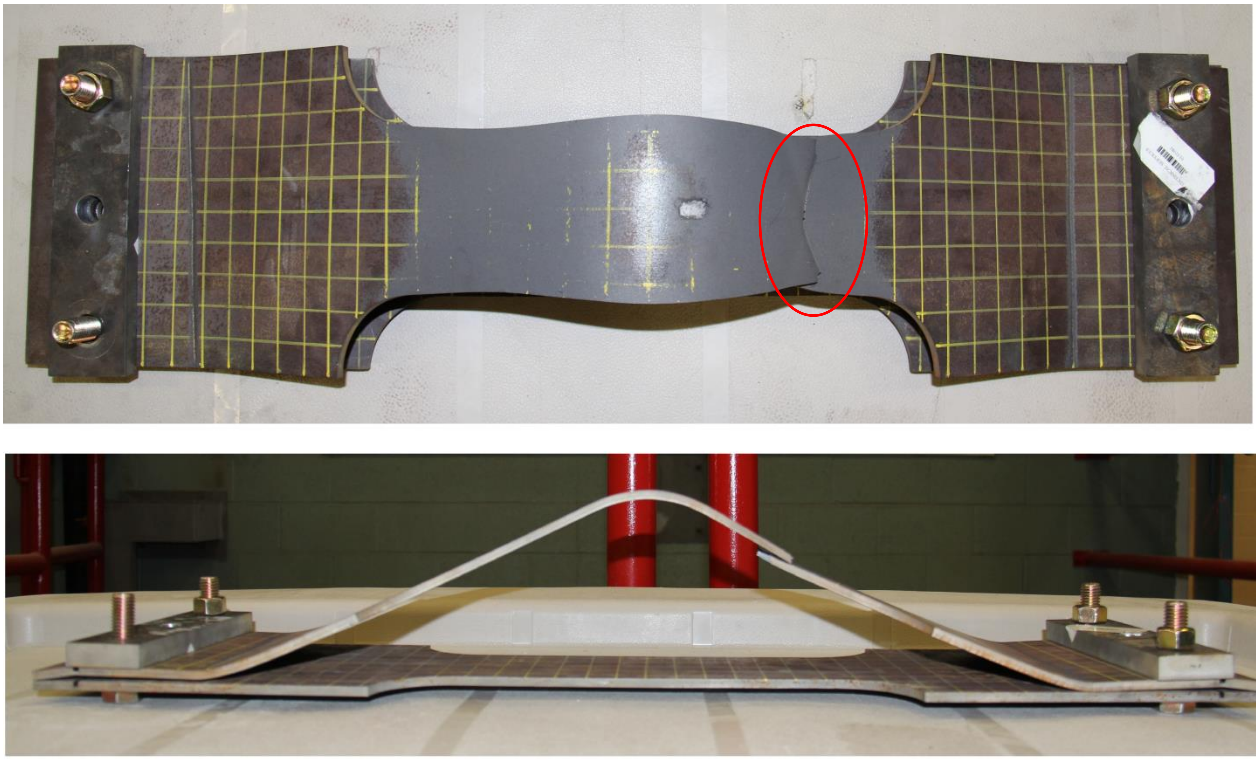

Figure 3-14: Crack path and the deflection in the thick plate (Jamaly, 2014)

In all steel plates, crack initiated in the centre of the width of the plate in normal fracture mode and then, continues to the edges of the plates, which is called slant fracture. Normal fracture region and slant fracture region are presented for thin plates in Figure 3-15 and for thick plates in Figure 3-16. These sequences and the crack propagation are shown in the pictures taken from the bottom of the plates during the experiments, which are presented in Figure 3-17 for the thin plate and in Figure 3-18 for the thick plate.

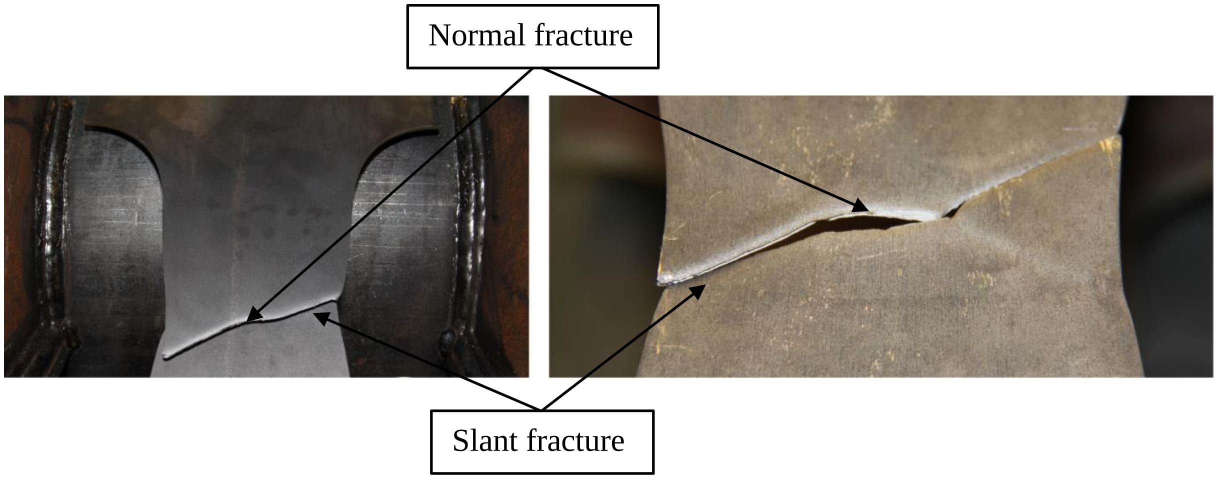

Figure 3-15: Normal and slant fracture in the thin steel plates

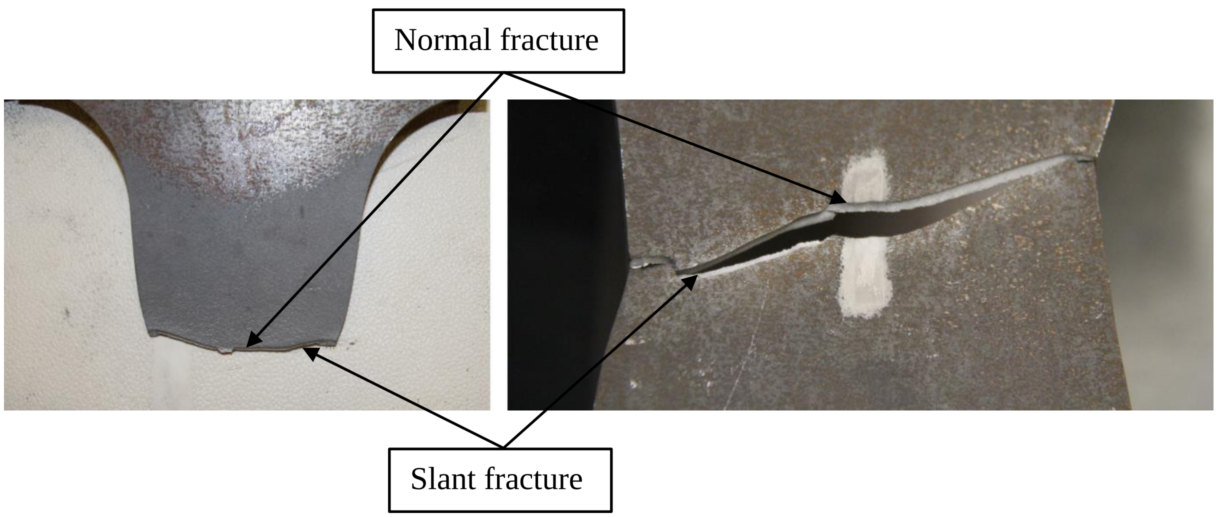

Figure 3-16: Normal and slant fracture in the thick steel plates

Figure 3-17: The sequences of the crack propagation in the thin plate (from left to right)

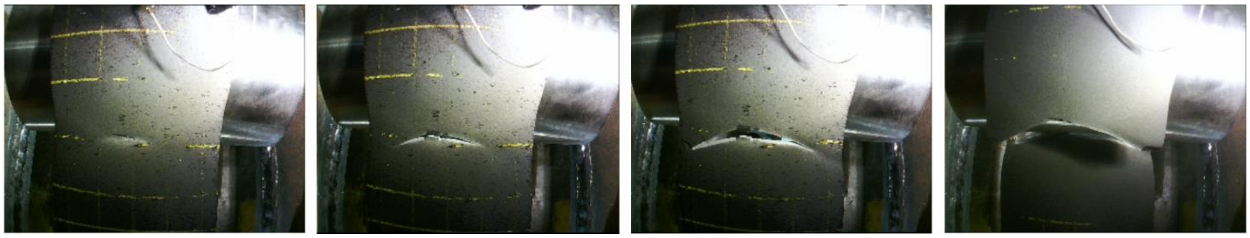

Figure 3-18: The sequences of the crack propagation in the thick plate (from left to right)

During the experiments, vertical force applied to the steel plates and the vertical displacement of the rigid indenter were recorded. The force-deflection curves for the thin and thick plates are depicted in Figure 3-19 and 3-20. Sudden falls in the curves are presenting the points at which the fracture in the steel plates happened. These curves will be compared to numerical results derived by using CZM in Chapter 4.

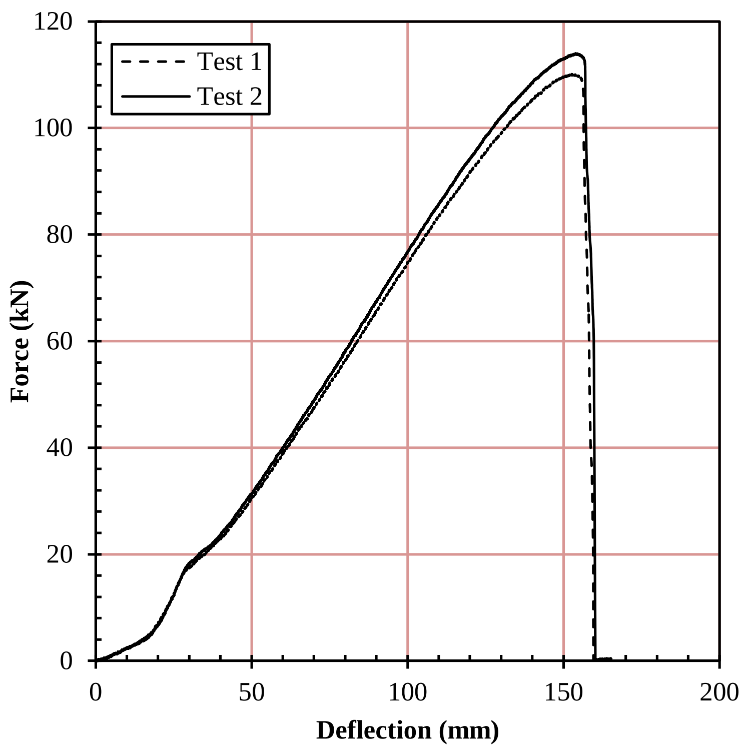

Figure 3-19: Force-deflection curves in thin plates- sudden fall shows the fracture (based on experiments done by Jamaly, 2014)

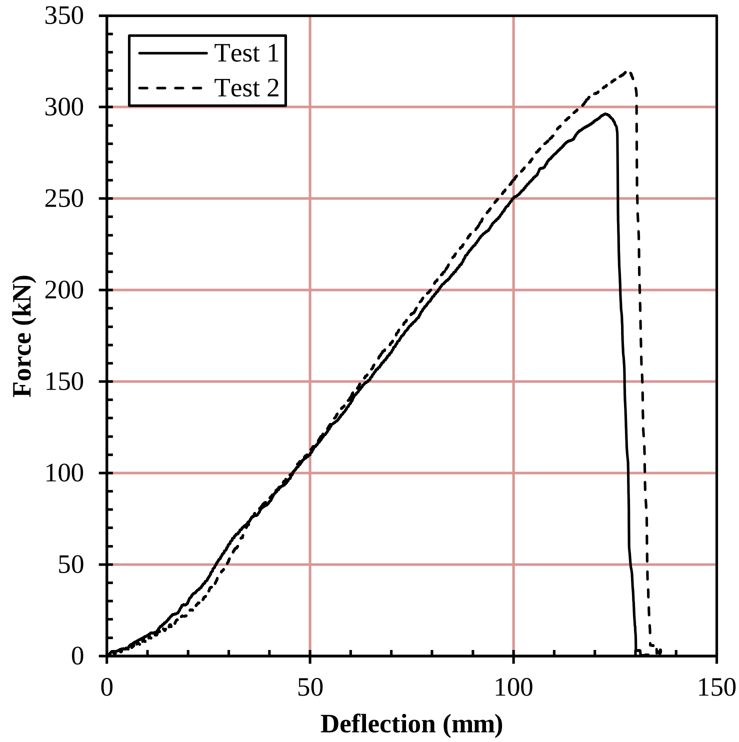

Figure 3-20: Force-deflection curves in thick plates- sudden fall shows the fracture (based on experiments done by Jamaly, 2014)

The force-deflection curves show a clear transition from plate bending towards membrane behavior. Prior to fracture, the force does not increase as the plate thinning, the necking phenomena, occurs. The necking continued until fracture happened. Fracture occurs very fast and this causes an immediate drop in force.

The horizontal distance of the crack locations from the plates' edge, for both thin and thick plates, are almost 300 mm. Figure 3-21 shows this distance on a sample of thick plates. These distances are presented in Table 3-2.

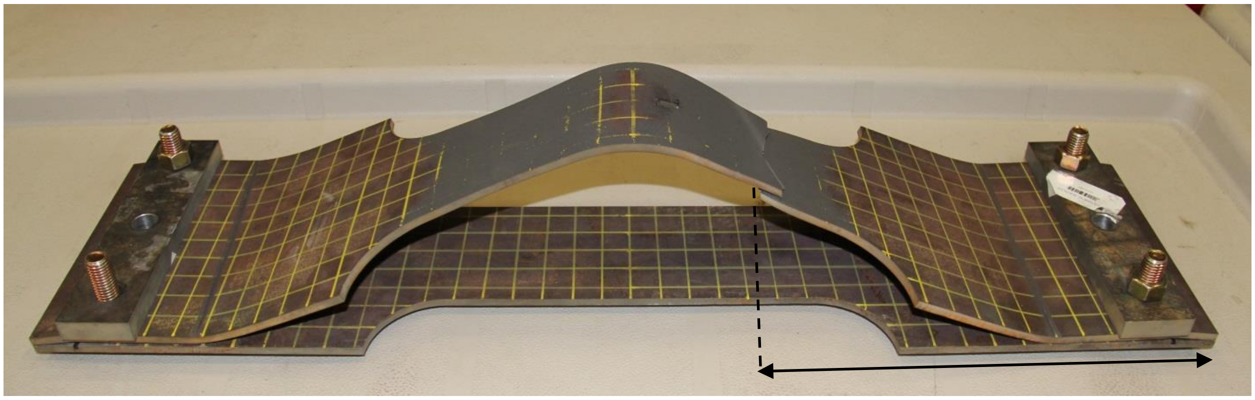

Figure 3-21: The horizontal distance of the crack locations (Jamaly, 2014)

Table 3-2: Crack location- horizontal distance from the edge of the steel plate

Specimen	Thin Plate Test No. 1	Thin Plate Test No. 2	Thick Plate Test No. 1	Thick Plate Test No. 2
Distance (mm)	320	310	325	330

Chapter 4: Finite Element Analysis

4-1. Introduction

This chapter describes the application of a 3D interface cohesive finite element model to predict quasi-static, ductile crack extension in steel for mode I loading and crack growth. The fracture model comprises initially zero thickness interface elements with constitutive response described by a traction-separation relationship. Conventional continuum finite elements model the elastic-plastic response of the main material. The interface cohesive elements undergo gradual decohesion between faces of the continuum elements to create new traction-free crack faces.

This part presents results from numerical analyses with focus on fracture prediction. The performance of CZM is investigated. In addition, the influence of the cohesive parameters with respect to onset of failure is studied.

In order to investigate the performance of the cohesive model under the same constraint conditions and the transferability of their parameters, tensile test simulations are used for parameter identification and calibration, and steel plate fracture tests simulation are used for cohesive model validation. It will be shown that for both models, a single set of parameters describes the mechanical behaviour of both types of specimens. A comparison of experimental results with those from FEA is carried out to assess the accuracy of the developed model.

For the entire investigation, ABAQUS is used.

4-2. Finite Element Analysis Basics

There are four main components in a finite element model:

- Analysis type

- Boundary conditions
- Material model
- Element definition

One choice that has to be made when planning Finite Element Analysis (FEA) is which method should be used to solve the problem numerically. Additionally, given the geometry of the considered problem, the modeller mainly has to decide on the boundary conditions, the material model, the mesh and the element type.

4-2-1. Analysis type

Generally, there are two methods to solve structural problems numerically: static analysis and dynamic analysis. The basic statement of static equilibrium is that the internal forces exerted on the nodes, I (resulting from the element stresses), and external forces, P, acting at every node must balance:

$$P - I = 0 \qquad \text{Eq. 4-1}$$

The major difference between static and dynamic analysis is the inclusion of the inertial forces, $M\ddot{u}$. Where, M is the mass and $\ddot{u}$ is the acceleration of the structure. A problem is dynamic when the inertial forces are significant and vary rapidly in time. Inertial forces are proportional to the acceleration of the mass in structure. The dynamic equilibrium equations are written for convenience with the inertial forces isolated from the other forces:

$$M\ddot{u} + I - P = 0 \qquad \text{Eq. 4-2}$$

This equation is simply newton's second law of motion. I and P may depend on nodal displacements and velocities but not any higher-order time derivatives. Thus, the system is second order in time, and damping/dissipation is included in *I* and *P*:

$$I = Ku + C\dot{u} \qquad \text{Eq. 4-3}$$

Where, *K* (stiffness) and *C* (damping) are constant, the problem is linear.

Solving a dynamic problem may require the integration of the equations of motion in time. The method used to integrate these equations through time, distinguish Abaqus/Standard and Abaqus/Explicit.

Abaqus/Standard is a general-purpose finite element program. It can solve both static and dynamic equilibrium equations. Implicit method, which requires direct solution of a set of matrix equations to obtain the state at the end of the increment, is used by Abaqus/Standard. Time increment size is not limited; generally, fewer time increments required to complete a given simulation. In order to solve nonlinear problems, iterations are required. Each time increment is expensive since each requires the solution for a set of simultaneous equations.

Abaqus/Explicit is a general-purpose finite element program for explicit dynamics. It solves highly discontinuous high-speed dynamic problems efficiently using explicit method. In explicit method, the state at the end of the increment depends solely on the state at the beginning of the increment, and Solution procedure does not require iteration. Time increment size is limited; generally, many time increments are required to complete a given simulation. Each time increment is relatively inexpensive because it is not required to solve a set of simultaneous equations.

Iteration is an attempt at finding the equilibrium solution in an increment. Abaqus/Standard uses an incremental-iterative solution technique based on the Newton-Raphson method. The method is unconditionally stable (i.e. any size increments can be used). Each increment usually requires several iterations to achieve convergence.

Abaqus/Explicit solution is conditionally stable and the size of the time increment must be controlled. Explicit methods generally require many more time increments than implicit methods for the same problem. In a nonlinear analysis, ABAQUS automatically chooses appropriate load increments and convergence tolerances and continually adjusts them during the analysis to ensure that an accurate solution is obtained efficiently.

Sometimes there are large inertia loads but can do static analyses because the loads vary slowly with time. Additionally, when the inertial or dynamic force is small enough, the equations reduce to the static form of equilibrium. In quasi-static problems:

- inertia forces are negligible,
- the velocity of the material in the test specimen is very small, and
- Kinematic energy is negligible.

In these problems, the energy history for a quasi-static problem would appear as shown in the Figure 4-1. The kinematic energy of the deforming material, E_K, does not exceed a small fraction of its internal energy, E_I, throughout the majority of the simulation. A small fraction typically means 1 to 5% (ABAQUS, 2010).

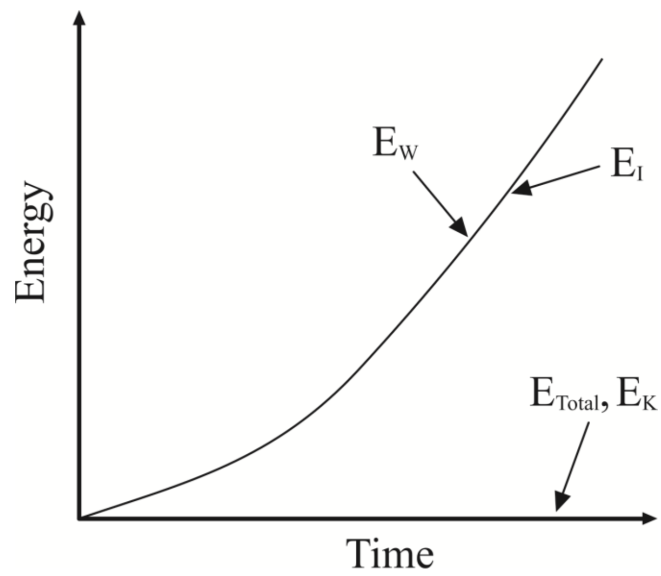

Figure 4-1: Energy history for quasi-static problem

In this research, Abaqus/Standard analysis method is chosen when analyzing the models because this can be an appropriate analyzing method to use in a quasi-static situation. Due to the relatively low velocity in ship collisions, the strain rate is low compared to other high-speed impact problems.

4-2-2. Nonlinearity

There are different kinds of structural nonlinearities. Sources of nonlinearity are:

- Material nonlinearities (including Nonlinear elasticity, plasticity, material damage, and failure mechanisms)
- Boundary condition nonlinearities (the boundary condition is not fixed and changes during the analysis. The most common example is the contact problem)
- Geometric nonlinearities (including large deflections and deformations, and large rotations)

Typical nonlinear problems have all three forms of nonlinearity. So the equilibrium equations must include the nonlinear terms; and generally, the nonlinear equations for each degree of freedom are coupled. All these nonlinearity types are present in the tensile test and the plate fracture test simulation. All of these structural nonlinearities are supported by ABAQUS.

When the displacements are small, the equilibrium equations can be established with reference to the initial configuration. When the ultimate strength of structures that collapse is to be calculated, the assumption about small displacements and linear material need to be modified. For a linear analysis, the stiffness matrix is assumed to be constant. In linear analysis following equation is solved in order to get the load or displacement

$$F = KU \qquad \text{Eq. 4-4}$$

Where, F is external load, U is nodal displacement, and K is stiffness matrix found from the linear strain stress relationship and is constant throughout the analysis.

When the structure undergoes large deformations, the material is nonlinear, or the boundary conditions change during the analysis, the stiffness matrix changes with deformation and needs to be recalculated in each load step. The governing equations are nonlinear with respect to displacement and an incremental solution scheme is used for solution. In this case, Eq. 4-4 is modified as:

$$F = K(U)U \qquad \text{Eq. 4-5}$$

Where, stiffness $K(U)$ is not a constant rather depends on the displacement.

In general, the above equation is not possible to be solved analytically. Normally incremental or iterative method is used. Then, Eq. 4-5 is expressed as:

$$dF = K(U)dU \qquad \text{Eq. 4-6}$$

Where, $K(U) = dF/dU$ is incremental stiffness; and dF and dU are corresponding increments in load and displacement, respectively.

With a given condition (U, F), K can be calculated and the displacement increment, dU, due to load increment, dF, can be calculated by following equation:

$$dU = K^{-1}dF \qquad \text{Eq. 4-7}$$

Nonlinear problems are generally solved in an incremental solution schemes. For a static problem a fraction of the total load is applied to the structure and the equilibrium solution corresponding to the current load level is obtained. The load level is then increased (i.e. incremented) and the process is repeated until the full load level is applied.

In static problems, the total load applied is broken into smaller increments so that the nonlinear solution path may be followed. In dynamic problems the total time period is broken into smaller increments to integrate the equations of motion. For a dynamic problem, the equations of motion are numerically integrated in time using discrete time increments. As mentioned, there are two different methods offered by ABAQUS to perform dynamic analysis, each of them with advantages and disadvantages depending on the considered problem: Abaqus/Standard and Abaqus/Explicit.

4-3. Modeling damage in ABAQUS

To help in understanding the fracture modeling capabilities in ABAQUS, consider the response of a typical metal specimen during a simple tensile test (the bilinear model is a reasonable and engineering model of the steel behavior). The stress-strain response, such as that illustrated in

Figure 4-2, will show distinct phases. The material response is initially linear elastic, AB, followed by plastic yielding with strain hardening, BC. Beyond point C there is a marked reduction of load-carrying capacity until rupture, CD. The deformation during this last phase is localized in a neck region of the specimen. Point C identifies the material state at the onset of the damage and damage initiates from this point. Beyond this point, the stress-strain response CD is governed by the evolution of the degradation of the stiffness in the region of strain localization. In the context of damage mechanics, CD can be viewed as the degraded response of the curve CD', which the material would have followed in the absence of damage.

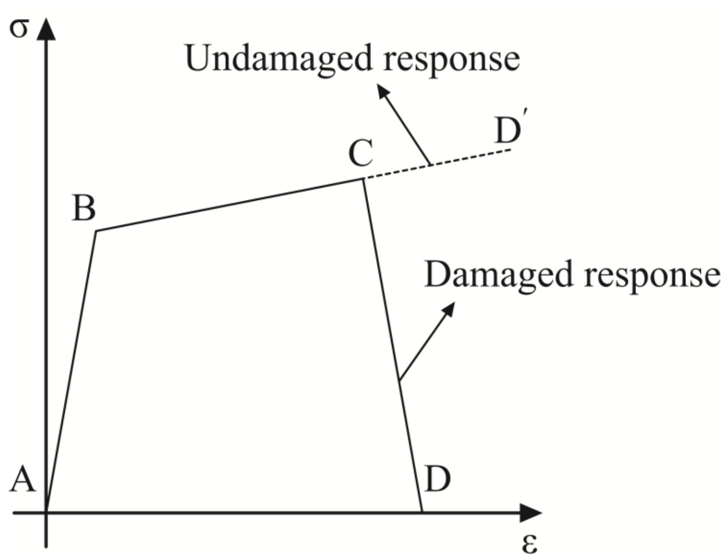

Figure 4-2: Typical material response showing progressive damage

Thus, in ABAQUS the specification of a failure mechanism consists of four distinct parts: (ABAQUS, 2010)

- the definition of the effective (or undamaged) material response (e.g. elastic-plastic material with hardening, ABCD' in Figure 4-2),
- a damage initiation criterion (e.g. C in Figure 4-2),

- a damage evolution law (e.g. CD in Figure 4-2), and
- material separation once the material stiffness is fully degraded (e.g. D in Figure 4-2).

All four components should be in material definition to model fracture. The strain softening part of the curve cannot represent a material property. Because it depends on fracture mechanics considerations and mesh size. In this research, ABCD' in Figure 4-2 is used as the material model of the continuum elements; and to address the strain softening issue, Cohesive Zone Model, with a bilinear TSL (Figure 2-4 a), is used.

ABAQUS has capability of predicting crack propagation. Element deletion technique is provided such that the element, where the failure criterion is locally reached, will be removed from the calculation. Thereby dynamic element deletion can be visualized as crack propagation. If a critical initiation value of some fracture parameter is exceeded, a crack starts to grow. Crack growth can also be simulated using node release techniques, controlled by any fracture mechanics parameter (e.g. J-integral) which requires knowing the crack location in advance. These two mentioned techniques are highly mesh sensitive and cause numerical convergence problems.

Modeling Cracks and crack-like defects induce high stress and strain gradients which require a fine mesh size resulting in large numbers of elements and degrees of freedom. Nonlinear simulations of components with stress concentrators are therefore expensive with respect to computation time and memory. All possibilities to reduce the number of degrees of freedoms should hence be utilized like:

- restricting to two-dimensional models of the structure if physically meaningful,
- coarsening the mesh away from the defect,

- introducing symmetry conditions.

To solve the mentioned problems in using Element deletion technique and node release technique, and the problems regarding the validity of classical Fracture Mechanics, CZM can be used. ABAQUS can handle crack using cohesive zone model, which is expected to be less mesh sensitive.

4-3-1. CZM in ABAQUS

To model fracture, in a finite element representation of CZM, cohesive elements are introduced as interface elements between continuum elements at the boundaries of continuum elements (i.e. along pre-defined crack paths). They do not have an initial thickness but upper and lower surfaces are distinct with duplicated nodes, which can separate during loading. The damage occurs only in the interface elements which obey a constitutive equation named TSL explained in Chapter 2.

In the cohesive model, the damage evolution in the structure is decoupled from its inelastic deformation. Material separation occurs only in interface elements which have no volume in the undeformed state, but can open under loading, that is, the two sides of the interface can irreversibly separate, which describes the evolution of damage and finally (if separation is larger than δ_0) results in the failure of the interface element. Hence, the continuum elements are separated.

Two main approaches that can be used to embed cohesive elements in a FE model are: (ABAQUS, 2010)

- embedding one or more layers of cohesive elements in the mesh of an existing model using offset technique. Offset mesh can be created only from three-dimensional element faces. As a result, only hexahedral- and wedge-shaped cohesive elements can be created using an offset mesh.

- creating the analysis model using the geometry and mesh tools. The connection at the interface between the cohesive layer and the surrounding bulk material can be modeled by sharing nodes or by defining a tie constraint. The tie-constraint approach allows modelling the cohesive layer using a finer discretization than that of the bulk material and may be more desirable in certain modeling situations.

Cohesive elements have an orientation associated with them. This orientation defines the thickness direction of the elements, and it should be consistent throughout the cohesive layer. Swept or offset meshing techniques should be used to generate the mesh in the cohesive layer, because these tools produce meshes that are oriented consistently. A single layer of solid elements should be created to model the cohesive region. The use of more than one layer through the thickness could produce unreliable results and is not recommended. (ABAQUS, 2010)

TSL consists linear elasticity with damage. Linear elasticity defines behavior before the initiation of damage. It relates nominal stress to nominal strain (nominal traction to separation with default choice of unit thickness). In ABAQUS, nominal stress and strain quantities are used for the traction separation law. If unit thickness is specified for the element (in section module, not in geometry), then the nominal strain corresponds to the separation value. If a non-unit thickness (h) is specified for the cohesive element, the value of the stiffness must be scaled accordingly:

$$E = h.K \qquad \text{Eq. 4-5}$$

ABAQUS requires that the cohesive elements thickness, h, and ten material parameters are inputted:

- Elastic stiffness (E_n, E_t, E_s),
- Damage initiation criterion (N_{max}, T_{max}, S_{max})
- Damage evolution (η, G_{IC}, G_{IIC}, G_{IIIC})

Assuming the isotropic behavior, $G_{IC} = G_{IIC} = G_{IIIC} = G_{TC}$; and for BK mixed mode behavior (Benzeggagh and Kenane, 1996), this makes the response independent of η term. Cohesive elements thickness are essentially zero in the geometry, but the cohesive section property thickness is specify as $h=1$, so nominal strains=separation and elastic modulus=stiffness. Isotropic behavior also implies the following:

- E_n,$=E_t$,$=E_s$ (equals to K, since $h=1$)
- $N_{max}=T_{max}=S_{max}=T_{ultimate}$

The traction-separation law is based on the separation between the top and bottom faces of the cohesive element. However, for considering symmetry condition, it should be noted that on a symmetry plane, the separation that computed is half of the actual value. TSL for considering symmetry condition is shown in Figure 4-3.

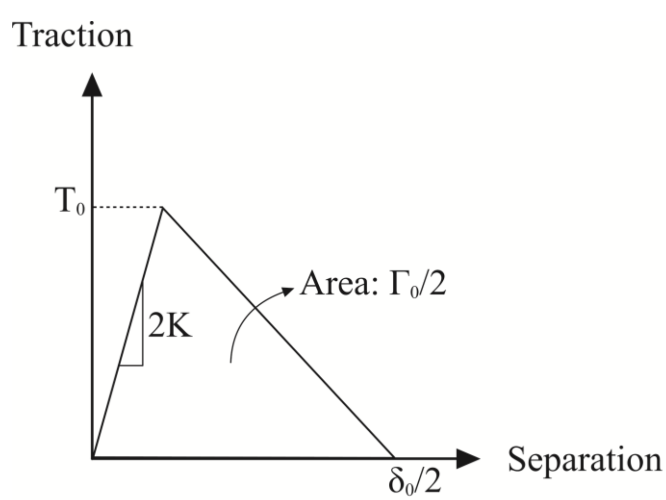

Figure 4-3: TSL for considering symmetry condition

While using cohesive elements, special issues should be considered that are specific to these elements. Such issues include special considerations associated with using cohesive elements in conjunction with contact interactions, and potential convergence problems in Abaqus/Standard.

4-4. Tensile Test Simulation

In order to derive and calibrate the cohesive material, numerical simulation of tensile specimens under tensile loading is performed using ABAQUS. Here, the finite element analysis of the test specimens studied in Chapter 3 is described.

For embedding cohesive elements in an existing three-dimensional mesh the solid offset mesh tool is used. For this approach, the offset distance is set to be zero to generate a layer of zero thickness hexahedral elements (with consistent orientation) between continuum elements that share nodes with the surrounding bulk material.

The FE mesh of the tensile bars, tested in Chapter 3, is shown in Figure 4-4 and Figure 4-5. Mesh size is 1 mm. 72 layers of cohesive elements are embedded in the necking region. The FE model consists of 11577 3D solid elements and 3570 3D cohesive elements in planes normal to the applied load between each layer of continuum elements for the thin tensile bar; and it includes 23154 3D solid elements and 7038 3D cohesive elements for the thick tensile bar. Since the cohesive elements have zero thickness in the beginning, they are not visible originally, but they are highlighted in red in Figure 4-4 and Figure 4-5.

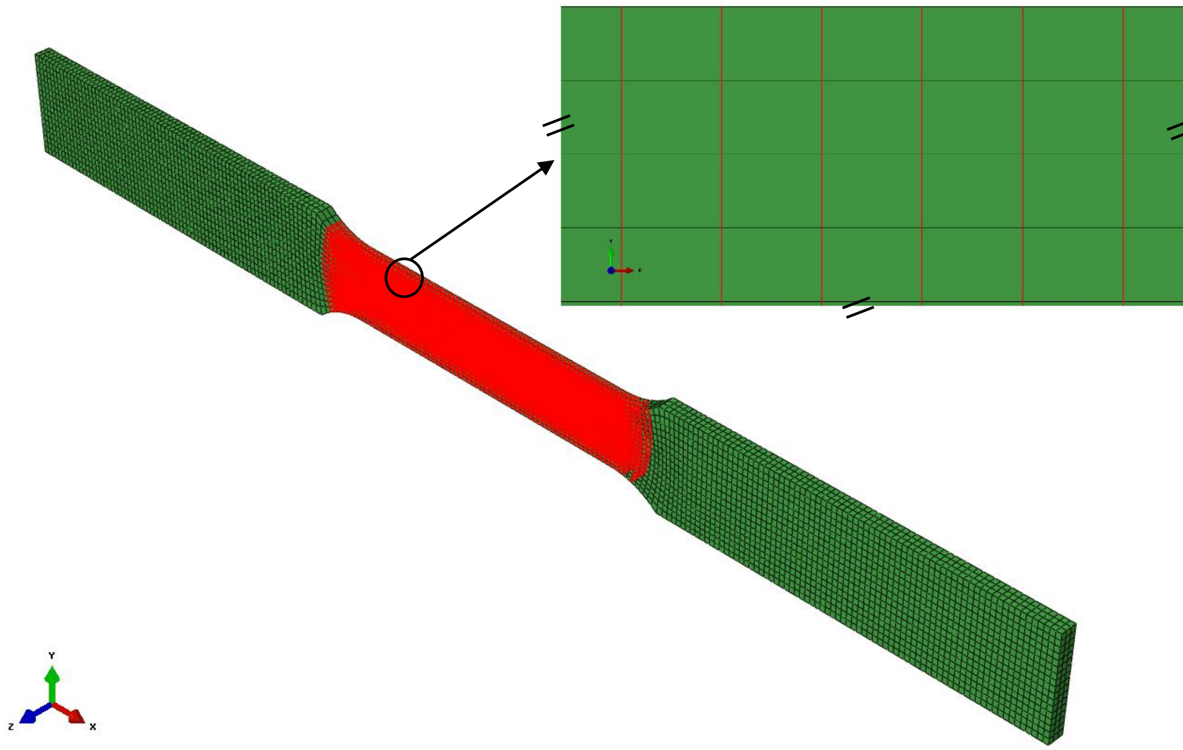

Figure 4-4: FE mesh of the thin tensile bar, 3.175 mm thickness. Cohesive elements are highlighted in red.

For FE simulation of the tensile tests, instead of applying tension forces to the both ends of the tension bar, a prescribed displacement is applied to both reference points at the two ends of tensile bar. Displacement-controlled loading allows the crack to grow in a stable fashion because the applied load is adjusted by increasing or decreasing it in order to maintain a certain rate of displacement, which is not possible under load-controlled loading. Thus, this phenomenon can be modelled statically, provided the applied displacement is below the amount that would cause dynamic crack growth. In a load-controlled experiment where the load is increasing or maintained at a certain value, the difference in the applied load and the required load increases monotonically as the crack grows. Thus, the specimen will experience dynamic and catastrophic failure. Such a phenomenon cannot truly be modeled in a static simulation. (ABAQUS, 2010)

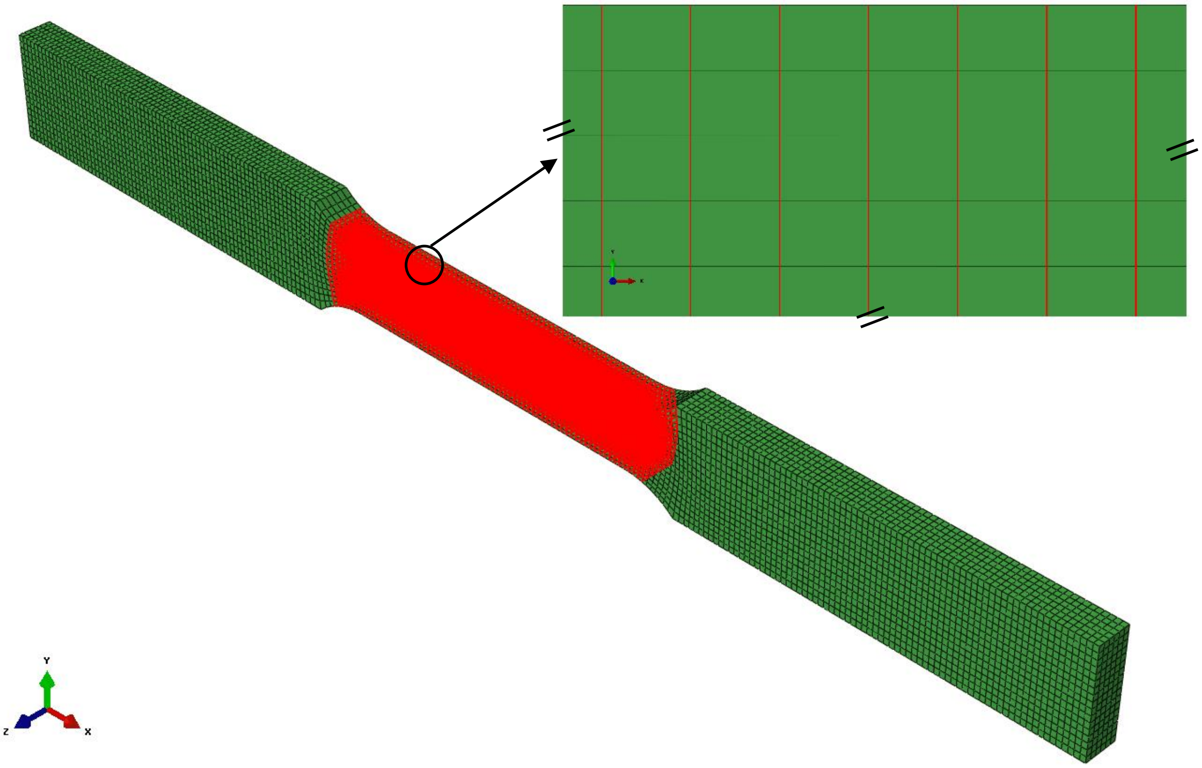

Figure 4-5: FE mesh of the thick tensile bar, 6.35 mm thickness. Cohesive elements are highlighted in red.

As mentioned, in FE simulation using cohesive modeling, the mechanical constitutive responses are classified to be based on:

- a continuum description of the material (for elastic-plastic material),
- a TSL of the interface material (for cohesive material)

The derivation of both material models are explained thoroughly in the following.

4-4-1. Stress- Strain Material Model

The stress and strain relationship for a material is a way to define how a material will react mechanically to an applied loading condition. In ABAQUS, the properties of a material for continuum elements is inputted as the relationship between true stress and true strain for the plastic straining, and the Young's modulus and the Poisson's ratio define the linear-elastic behavior leading to the plasticity. The material model in FEA is determined by tensile tests on steel flat bars explained in Chapter 3. Typically, the material behaviour of steel in FEA can be idealised as bilinear model with elastic and linear strain hardening components. The slope at elastic region is represented by Young's Modulus.

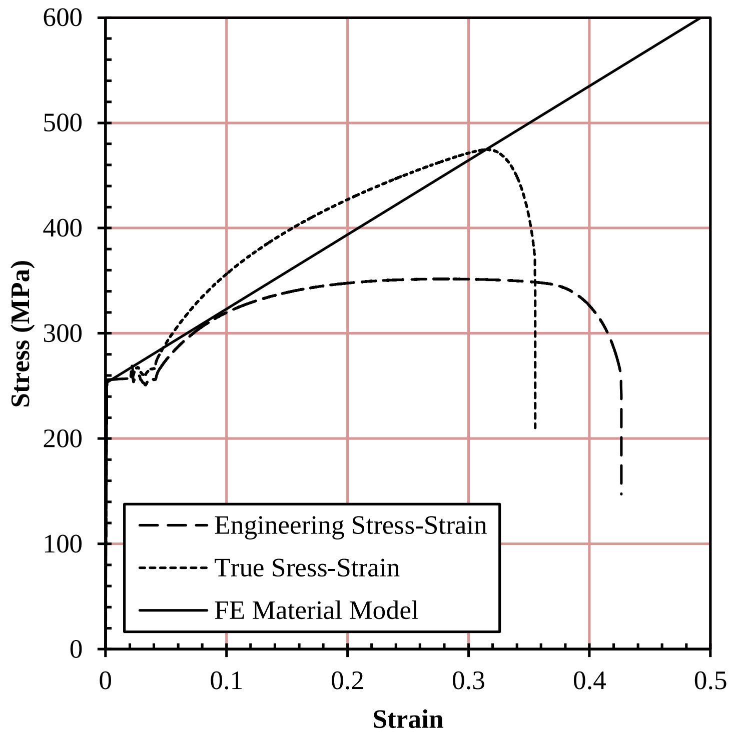

Figure 4-6: Engineering stress-strain curve, true stress-strain curve, FE bilinear curve for 3.175-mm plate

For the generation of a stress–strain curve, the engineering values from the tensile tests, given in Figure 3-6 and 3-7, first were converted to true stress- true strain values. Since the yield stress and the ultimate stress (the point at which fracture starts) on the stress-strain curve are the most important points, this curve is idealized as a bilinear curve which is then used for all subsequent numerical simulations. These curves are shown in Figure 4-6 for specimens with 3.175 mm thickness and in Figure 4-7 for specimens with 6.35 mm thickness. The elastic properties are given in Table 3-1. These materials are used for modeling the mechanical behavior of the continuum elements. This is an approximation of the material's behaviour. Therefore, the results of the FE simulation should be also discussed with respect to the choice of the stress-strain curve.

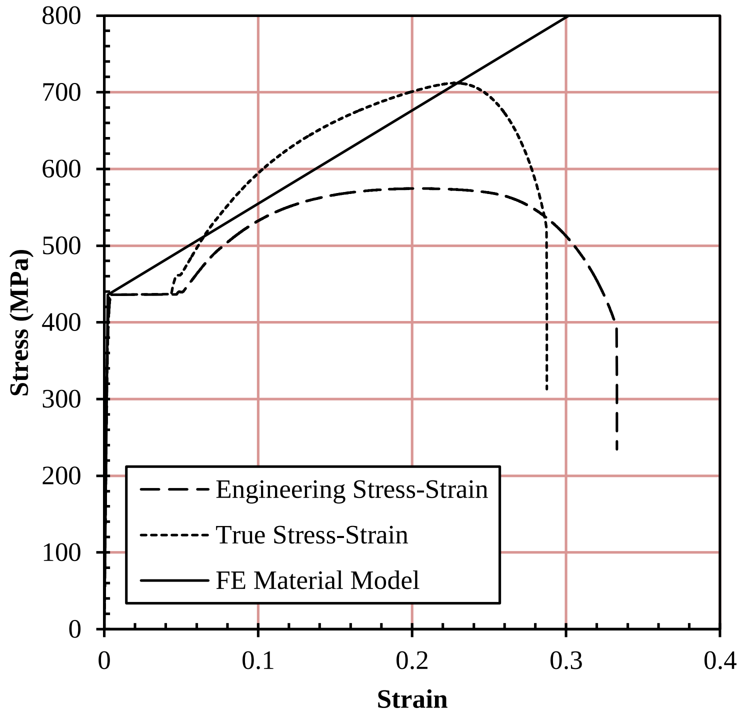

Figure 4-7: Engineering stress-strain curve, true stress-strain curve, FE bilinear curve for 6.35-mm plate

4-4-2. Traction- Seperation Material Model

As mentioned, in order to derive the FE material model including elastic-plastic material for continuum elements and TSL for cohesive elements, the tensile tests were done. Calibration tests of the fracture parameters in cohesive elements are conducted by modeling uniaxial tensile tests in FE software and comparing the numerical and experimental results.

ABAQUS provides three types of TSL, including triangular, exponentially softening, and user defined softening models. The most popular model among these three traction-separation laws for cohesive element is triangular traction-separation law. It is simply defined with elastic stiffness (K), strength of an element (T_0), and either critical displacement at failure (δ_0) or fracture energy (Γ_0). In the triangular model, applied stress on cohesive element increases with the slope of K up to the strength of the element (T_0) and decays linearly till the displacement of the element reaches to critical displacement (δ_0). The critical energy release rate of this model can be easily calculated by getting the area under the traction-separation curve.

As explained in Chapter 2, an estimate of the cohesive strength, T_0, was obtained from the normal stress at fracture of the flat tensile specimen during the tensile test. The engineering stress at failure, as calculated by the force at failure divided by the original cross section of the specimen, was then set equal to the cohesive traction. The separation energy, Γ_0, was pre-estimated from the J-integral at crack initiation. Using Eq. 2-10 and the procedure explained in Chapter 2, cohesive energy is calculated. Generally, $\Gamma_0 \leq J_i$, and J_i can be taken as a first approximation for Γ_0 in a subsequent parameter fitting process. The definite values of the parameters can be determined in an inverse procedure by fitting simulation results to experimental records.

The cohesive parameters can be calibrated by simulations of the tensile test with cohesive elements through fitting numerical data to experimental data. Figure 4-8 and Figure 4-9 present the results of FEA simulation of the tensile bar tests for various combination of T_0 and Γ_0. Note that the different T_0 values did not change the load-displacement curve but only the point of failure. It is observed in the parameter study that T_0 determines the ductility of the specimen and the effect of the cohesive energy is much less than the effect of cohesive strength. If the strength of cohesive element is higher than the ultimate stress of the ductile steel plate, it will stay only in the elastic region, while if the strength is lower than the ultimate stress, the cohesive model will start to show softening behavior before the steel reaches its ultimate stress. Therefore, when using the cohesive elements, capturing the softening behavior of the ductile steel is really difficult.

The subsequent optimization of the parameters by simulations of the load-displacement curve yielded $T_0 = 335\,MPa$ and $\Gamma_0 = 250\,N/mm$ for mild steel and $T_0 = 555\,MPa$ and $\Gamma_0 = 410\,N/mm$ for high tensile steel. These values will be used to simulate fracture in the steel plate fracture tests.

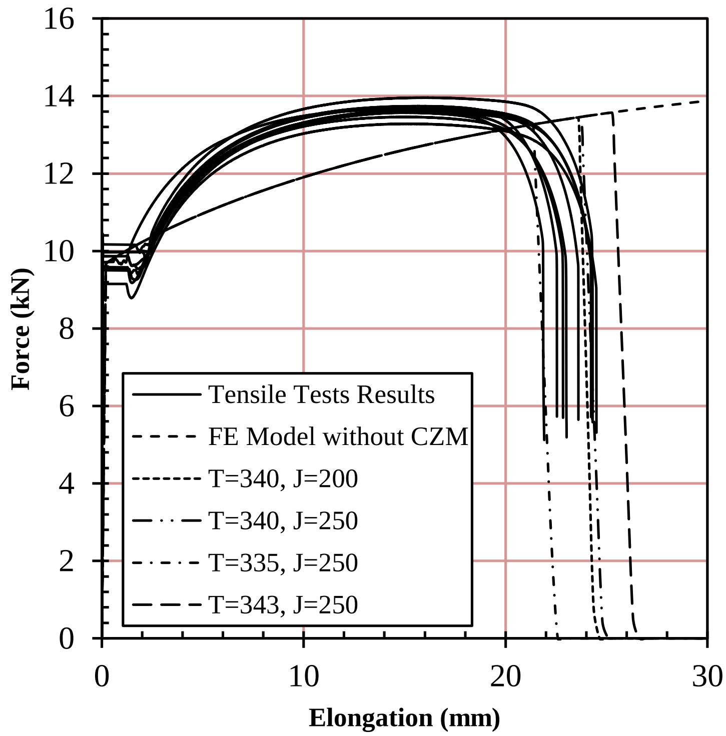

Figure 4-8: Determination of cohesive parameters for mild steel (3.175 mm thickness) and the effect of the variation of cohesive parameters on the fracture simulation

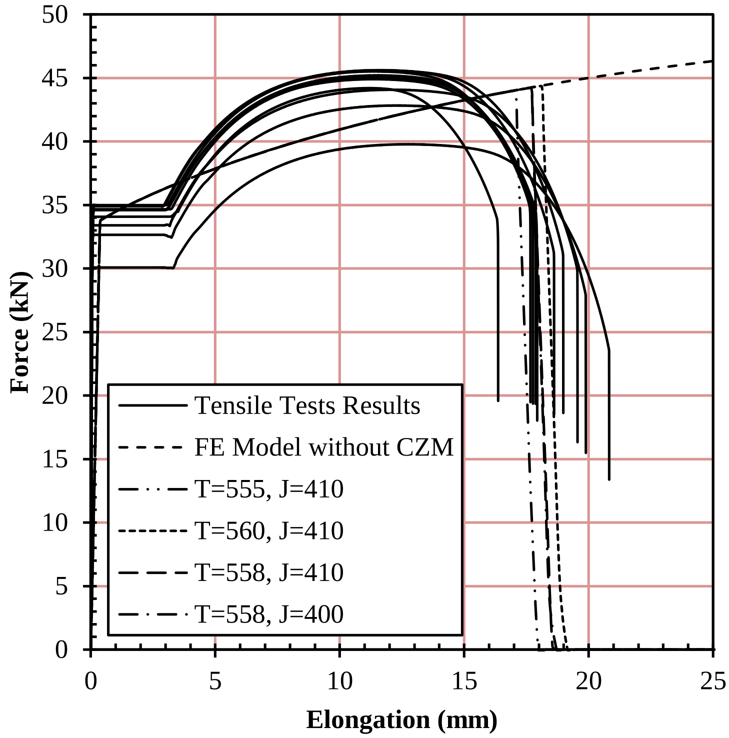

Figure 4-9: Determination of cohesive parameters for high tensile steel (6.35 mm thickness) and the effect of the variation of cohesive parameters on the fracture simulation

It should be mentioned that force-displacement curve in case of numerical simulation, even without modeling the damage (FE Model without CZM in Figure 4-8 and 4-9), has small deviation from experimental results. This is because of the fact that the FE model for the elastic-plastic material was idealized to a bilinear curve (to reduce simulation time significantly), while more accurate elastic-plastic material model may improve the numerical simulation results. The general behavior of load-displacement curve of numerical simulation compares well with the experimental results.

Even though the tensile specimen has a simple geometry and the loading is uniaxial, the mechanism of failure of that specimen is very complex due to the mixed fracture. In tensile test, fracture initiates in the center of the breadth of the specimen after significant plastic deformation with a pure normal fracture mode. Then, the normal fracture mode transits to a slant fracture mode of ductile tearing, where, the crack is inclined and propagate along approximately 45° angle to the surface of the specimen. The crack thus extends locally in a mixed-mode configuration. (Scheide et al., 2003; Cornec et al., 2009)

The numerical simulation of the fracture behavior of the tensile bar using the cohesive model is considered successful if numerical load-deflection curves agree well with the experimental load-deflection curves and the following phenomena can be realized:

- The crack initiates in the center of the breadth of the specimen.
- The crack extends to the outer surface and deviates from the original crack plane into the 45° plane.

As mentioned, in the present study, slant fracture is treated like a mode I fracture (normal separation) with the fracture plane normal to the applied load and the appropriate effective cohesive parameters. The idealization of the cohesive model does not consider the real slant fracture (under 45° across the thickness). Crack propagation is modelled in the projection plane equivalent to normal fracture but with cohesive parameters consistently determined as well in the projection plane.

Interface cohesive elements are placed only in flat plane directions between the continuum elements, constraining crack growth in the flat plane directions (mode I fracture). Figure 4-10 and 4-11 show crack growth in cohesive elements. In FE simulation similar to the experiments, the crack initiates in the centre of the breadth of the tensile specimen and extends to the outer surface. In reality, after the normal fracture initiation in the middle of the specimen, the crack shoud extend to the circomference in 45 degree.

In this simulation, the cohesive elements were just inserted in perpendicular direction to the bar axis between the continuum elements. Hence, crack develops in a flat plane. Modeling of the transition from flat to slant local fracture modes, using interface cohesive elements, lies beyond the scope of this study. The numerical models restrict crack to propogate in flat mode only. The focus here lies on the numerical and experimental results comparison, and the overall capability of the models to predict the measured load-crack extension response. Exact features of the transition to local slant fracture likely involve a complex interaction between fracture parameters.

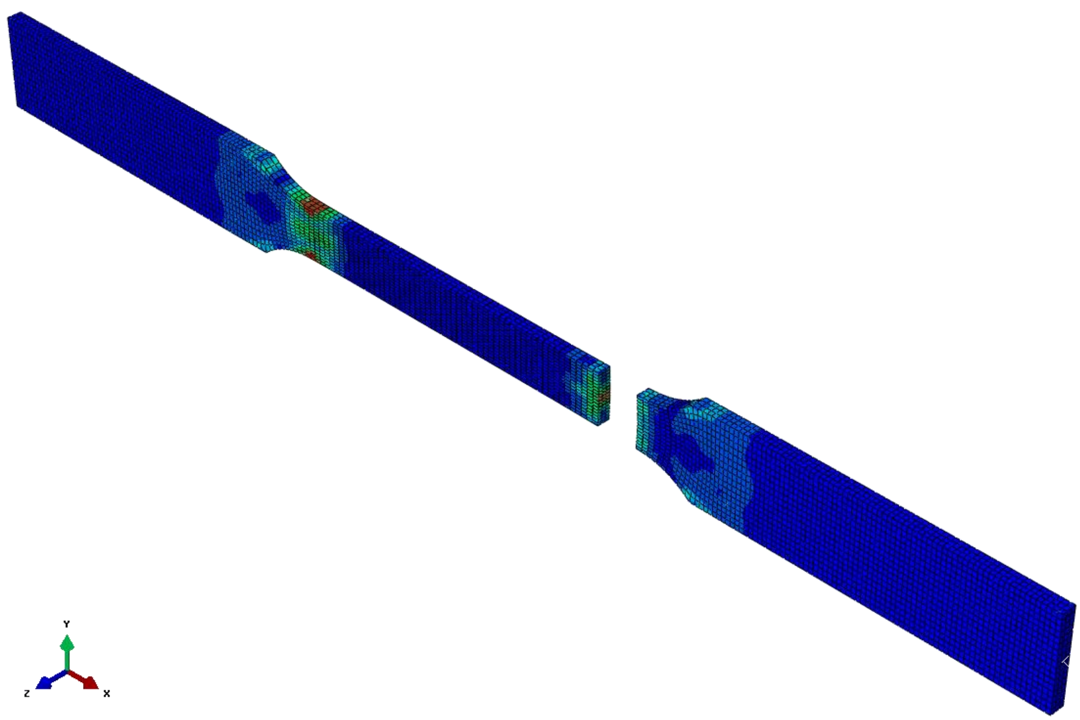

Figure 4-10: Crack growth path during the tensile test - 3.175 mm thickness

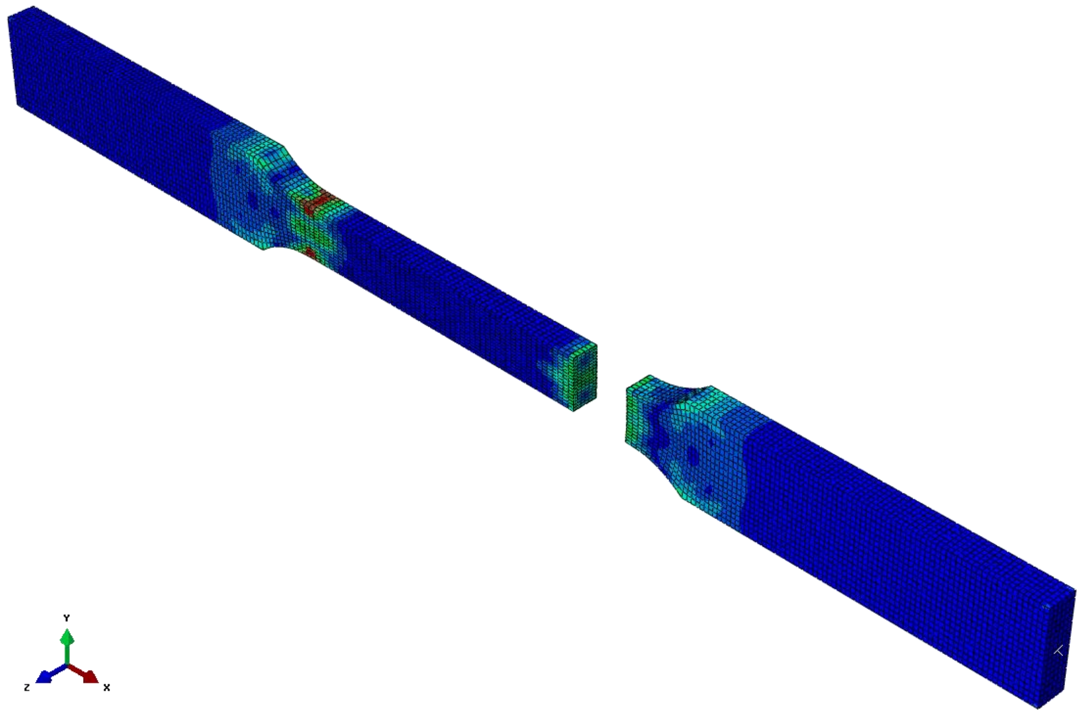

Figure 4-11: Crack growth path during the tensile test - 6.35 mm thickness

As described above, direct measurements of the respective quantities were combined with FE simulations of fracture mechanics tests for a fine-tuning of the parameters. The cohesive parameters such as fracture energy were calibrated, so that the elements fail at the appropriate value of applied load or displacement. These parameters are used to simulate steel plate fracture in next stage. Calibrated cohesive parameters are presented in Table 4-1.

Table 4-1: Cohesive parameters

Steel	mild steel	high tensile
Plate Thickness (mm)	3.175	6.35
T_0 (MPa)	335	555
Γ_0 (N/mm)	250	410

4-4-3. Convergence Studies

Mesh dependence of numerical results is a big issue in damage mechanics when softening behavior of material is simulated. As mentioned in Chapter 1, simulation of fracture using fracture criteria in FEA is highly mesh sensitive. On the other hand, since the cohesive law is expressed in terms of stress depending on the separation, a length scale parameter (characteristic length) is inherent to the model. In other words, a cohesive law introduces well-defined fracture energy (fracture or cohesive energy is the work of separation per unit area). Thus, no mesh dependence is expected and finite element models with cohesive elements are mesh independent, which is always a big issue in application of fracture criteria in FEA.

In this part, fracture simulation with two different mesh sizes, but with the same cohesive parameters, is conducted to investigate the fracture in both thin and thick tensile specimens. The tensile test simulation is repeated with 2 mm and 4 mm mesh size. Finite element model of the tensile bars, after the fracture, are shown in Figure 4-12, 4-13, 4-14, and 4-15.

The numerical results are presented in Figure 4-16 and Figure 4-17. As it was expected, mesh size does not have a significant effect on the final results when cohesive elements are used for fracture analysis. The prediction of the fracture point using CZM is less mesh sensitive in comparison with the other FEA techniques to analyze fracture. This is one of the advantages of the CZM, which reduces the simulation time significantly.

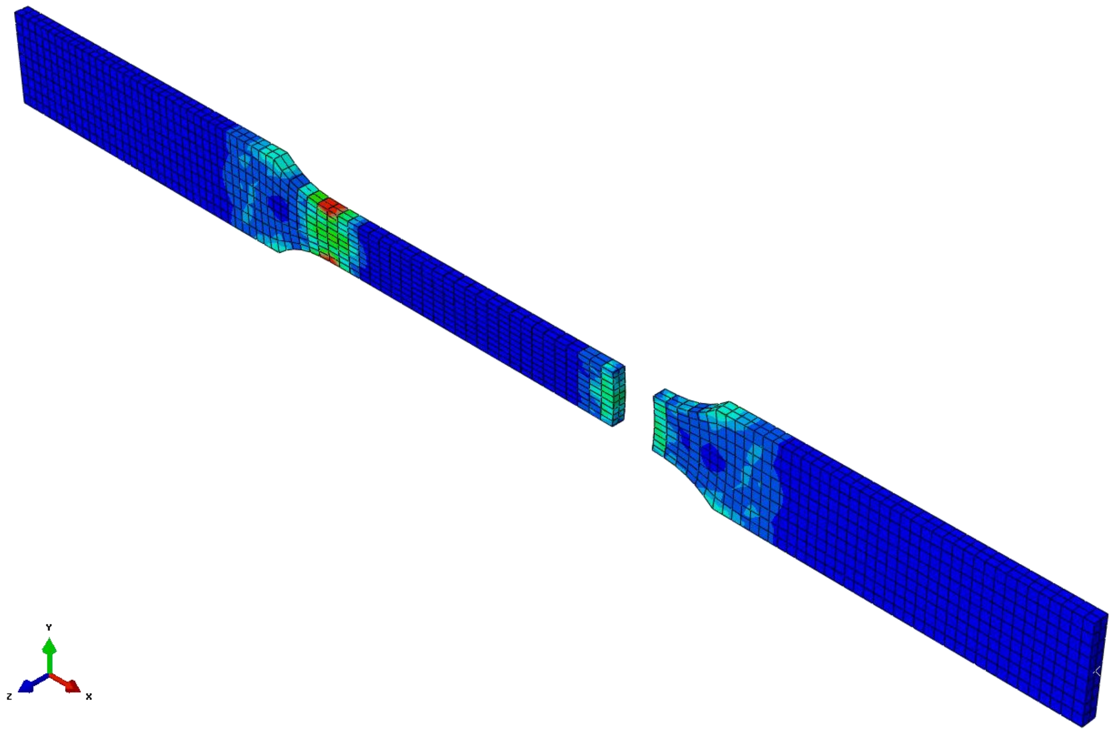

Figure 4-12: Crack growth path during the tensile test, 3.175 mm thickness, 2 mm mesh size

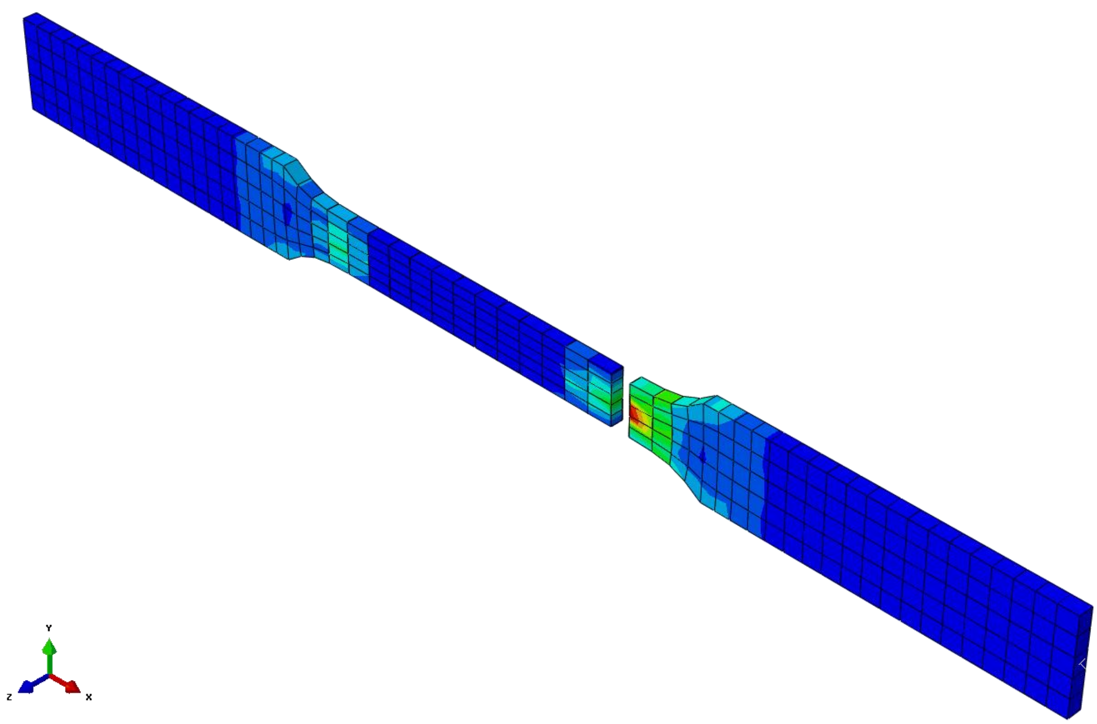

Figure 4-13: Crack growth path during the tensile test, 3.175 mm thickness, 4 mm mesh size

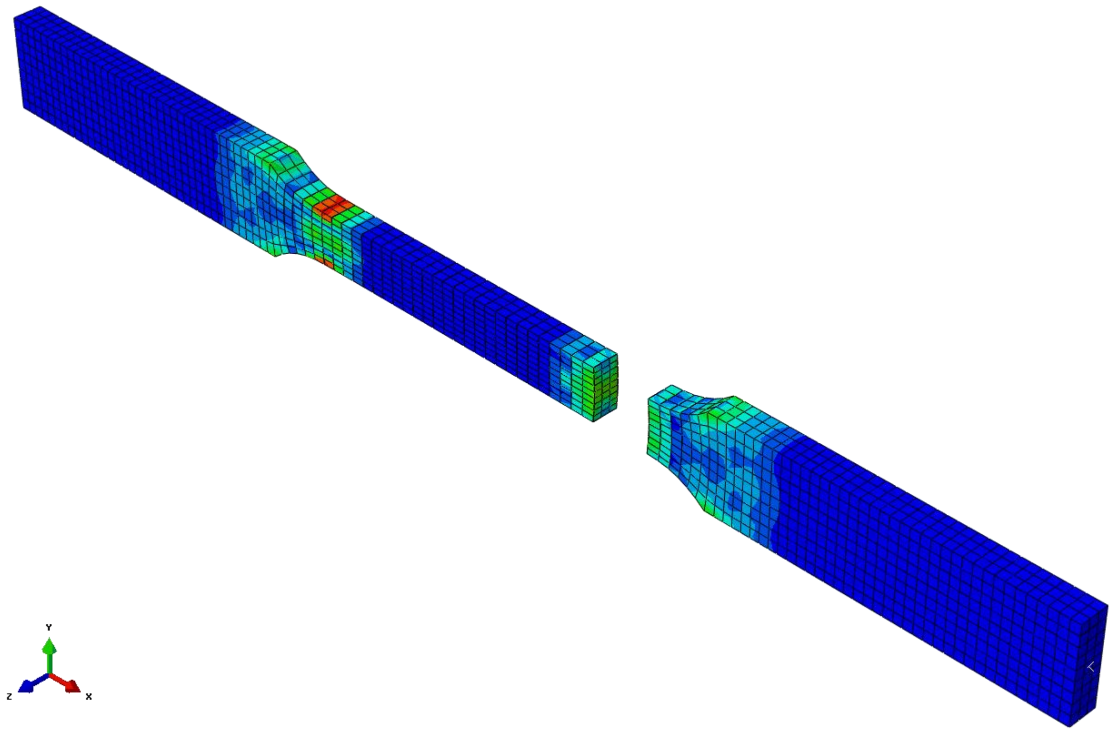

Figure 4-14: Crack growth path during the tensile test, 6.35 mm thickness, 2 mm mesh size

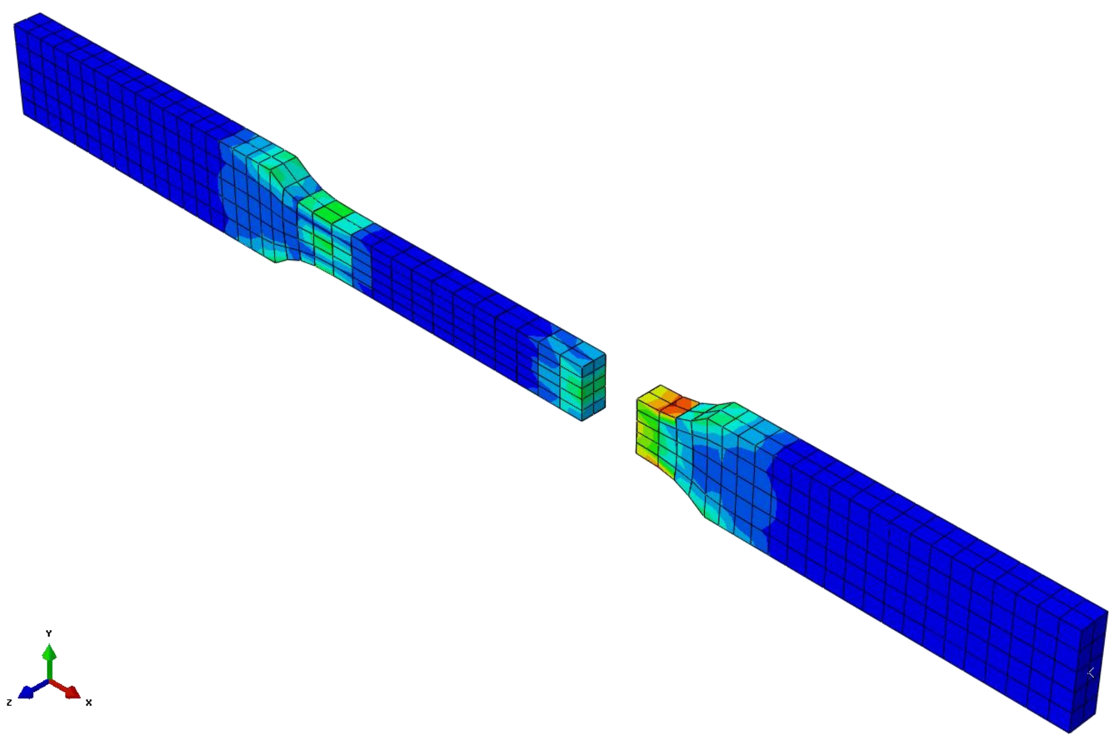

Figure 4-15: Crack growth path during the tensile test, 6.35 mm thickness, 4 mm mesh size

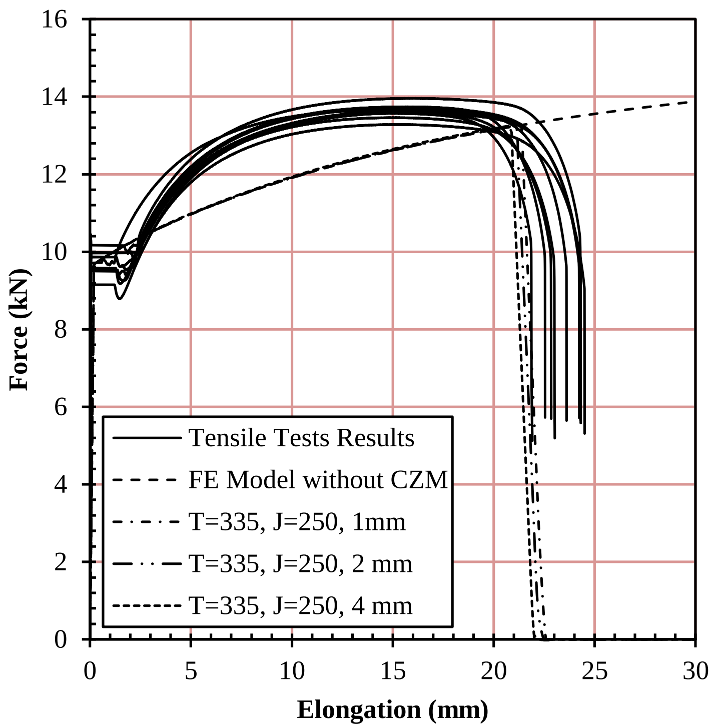

Figure 4-16: Load-elongation curve of the tensile test for 3.175 mm specimen

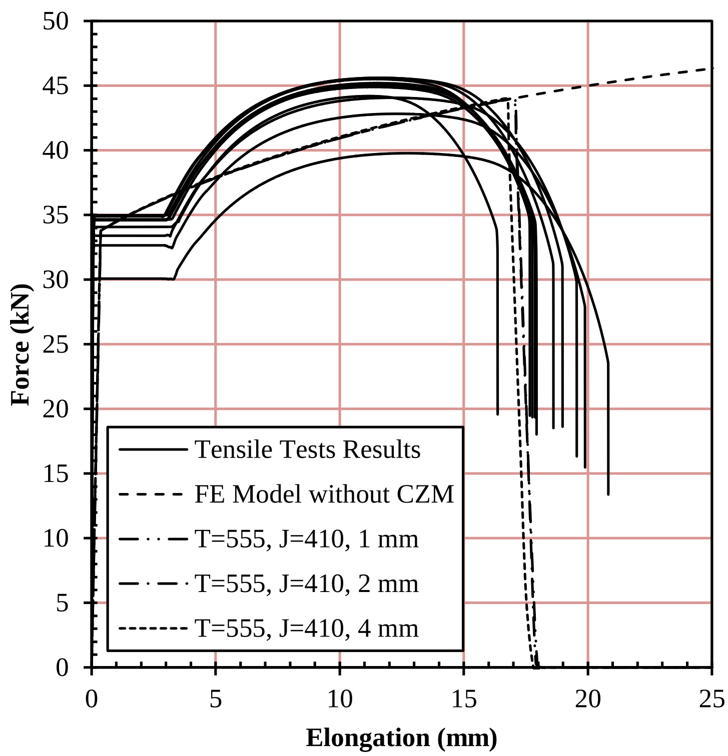

Figure 4-17: Load-elongation curve of the tensile test for 6.35 mm specimen

4-5. Plate Fracture Test Simulation

The transferability of the cohesive model parameters to other specimen sizes and geometries is investigated in this part. Experimental results of the steel plates loaded by rigid indenter (presented in Chapter 3) are used to validate the cohesive model transferability to other specimens with the same stress triaxiality.

The plate fracture test setup and the required dimensions were illustrated in Figure 3-10, Figure 3-11 and Figure 3-12. In order to numerically simulate these experiments and investigate crack initiation and propagation in the steel plates, the test setup is modeled in ABAQUS.

In ABAQUS, problems with multiple components are modeled by associating the geometry defining each component with the appropriate material models and specifying component interactions.

The indenter was modeled as a discrete rigid surface. This means that the surface of the indenter will not be able to deform, and will keep its initial shape throughout the analysis. The discrete rigid surface is defined by a mesh of undeformable elements. Having elements containing nodes is beneficial when the contact between the surfaces of the two parts are to be defined. This saves computation time when running the analysis.

Alternatively, an analytical rigid surface could have been used. This is a rigid surface that is defined by the geometry, and not a mesh of rigid elements as the discrete rigid surface. This will make the computer analysis run more slowly, since the geometrically defined surface is more complicated to analyze than the meshed surface of the discrete rigid body.

In order to ensure that the indenter moves down to the plate, perpendicular to the plate's initial surface, the reference point of the indenter was restrained against all movements and rotations except for the translation in the global y-direction, perpendicular to the plane of the plate. The contact between the outer surface of the indenter and the upper surface of the plate is defined using General contact.

Generally, there are three contact models in ABAQUS:

- General contact
- Node-to-Surface contact (Slave nodes cannot penetrate master surface segments. Nodes on the master surface can penetrate slave surface segments.)
- Surface-to-Surface contact

The two contact algorithms, however, can be used together in the same analysis. The General contact algorithm automatically avoids processing interactions that are treated by the contact pair algorithm. Here, General contact is used for the whole model, and beside defining the General contact, in order to model the contact between the indenter and the cohesive elements of the plate more precisely, Node-to-Surface contact is used.

For modeling contact, the slave surface should be meshed more finely than the master surface. If mesh densities are equal, the slave surface should be the surface with softer underlying material. (ABAQUS, 2010) Here, the plate's mesh size is 2 mm, the mesh size of the indenter and the boundary plates is 4 mm. the plate is also softer than the indenter and the boundary plates.

It should be mentioned that the other reason that in this research, discrete rigid is used is the fact that analytical rigid surfaces are not currently supported by General contact model in ABAQUS. Discrete rigid bodies can be used with both general contact and contact pairs.

Additionally, two curved plates in the test setup, which are assumed to be rigid and fixed, are modeled. Another contact between the rigid plates and the plate under investigation is defined.

The bolts used to attach the plate to the boundary plates are not modeled and the ends of the plate under investigation are attached to the boundary plates using tie constraint to model rigid boundary condition.

Output was requested for the displacement and the reaction force in the reference point of the indenter. These are used to evaluate the analysis against the force-displacement curves that were developed in the plate fracture tests.

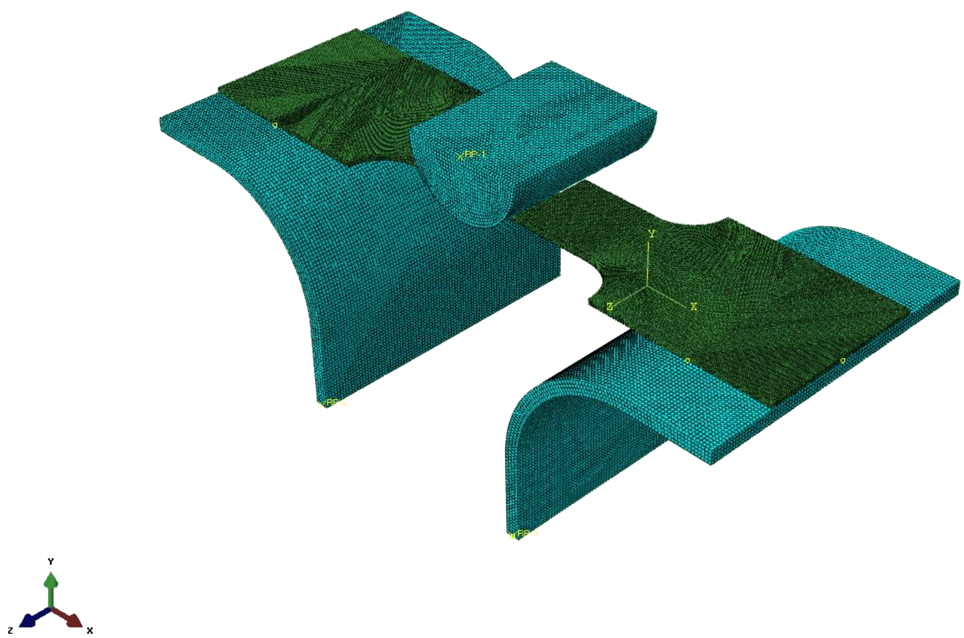

Figure 4-18: FE model of the plate fracture test

Cohesive elements are embedded between continuum elements. The FE model of the thin plate fracture test consists 50142 3D solid elements and 5304 cohesive elements. The FE model of the thick plate fracture test with 75192 3D solid elements and 9300 cohesive elements is shown in Figure 4-18. The mesh size for the steel plate is 2 mm and for the rigid indenter and the rigid plates are 4 mm. A layer of cohesive elements is embedded between each two layers of continuum elements in necking region perpendicular to the plate surface. Zero thickness cohesive elements are not visible originally, but they are highlighted in red in Figure 4-19 and Figure 4-20 for illustration purpose.

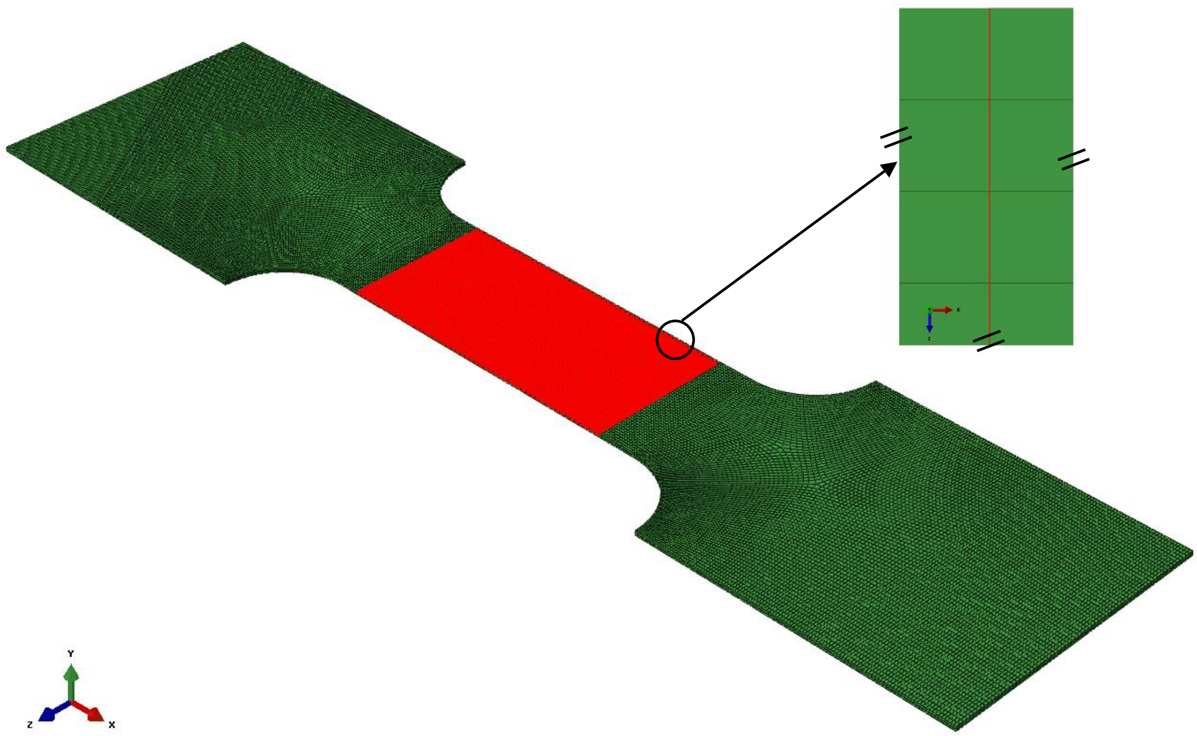

Figure 4-19: FE mesh of the steel plate with 3.175 mm thickness. Cohesive elements are highlighted in red.

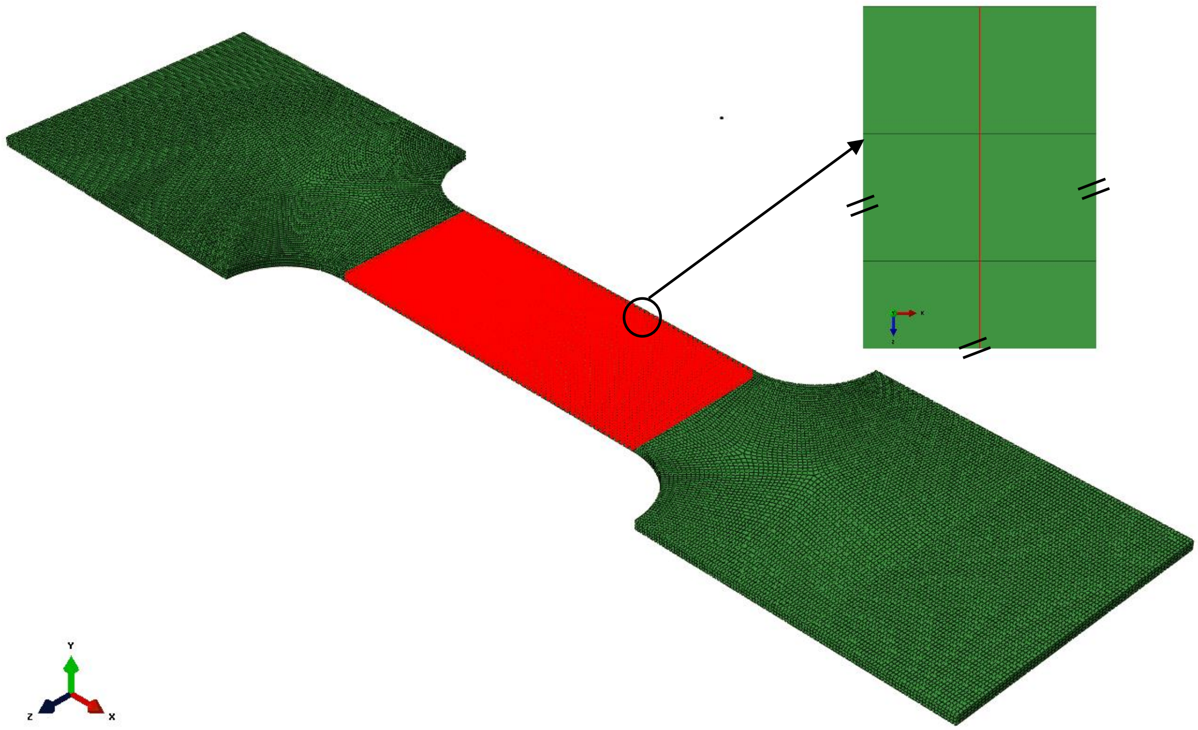

Figure 4-20: FE mesh of the steel plate with 6.35 mm thickness. Cohesive elements are highlighted in red.

The rigid indenter will push the plate downward until fracture happens. In the numerical simulation of the plate fracture, the same as in the plate fracture experiments, the crack starts in the centre of the breadth of the plate and grows to the surfaces of the specimen, which shows the capability of the CZM to model the exact crack propagation path. The crack propagations are presented in Figure 4-21 and Figure 4-22 (views from the bottom of the plates).

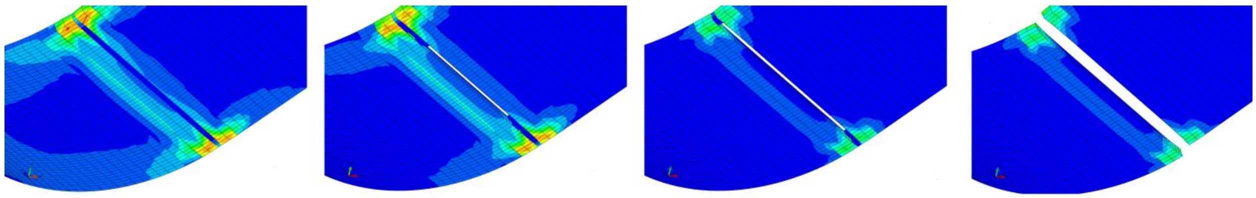

a)

b)

Figure 4-21: The sequences of the crack propagation a) in the FE model of the thin plate, b) in the experimental test of the thin plate (from left to right)

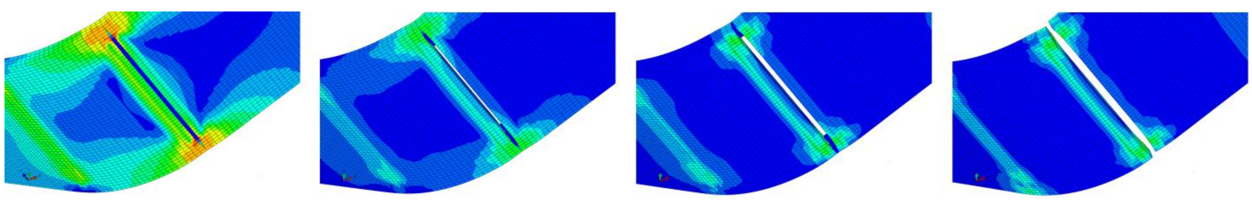

a)

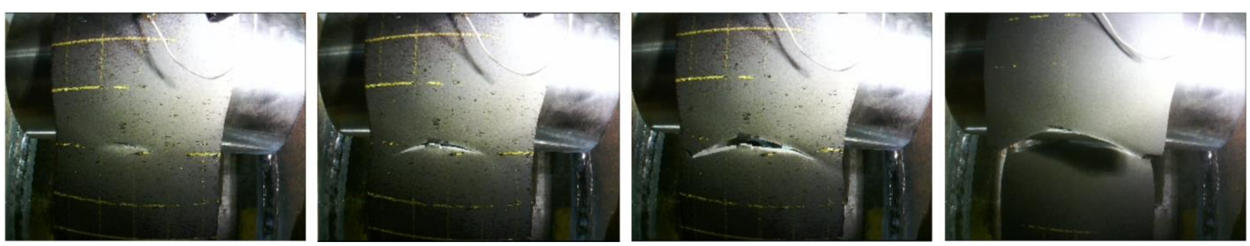

b)

Figure 4-22: The sequences of the crack propagation a) in the FE model of the thick plate, b) in the experimental test of the thick plate (from left to right)

The steel plates at the end of the simulation are presented in Figure 4-23 and Figure 4-24. The general crack path and the crack initiation point in the plates, simulated numerically, compare reasonably to Figure 3-13 and 3-14 from experimental tests. It should be mentioned that the crack path is restricted to propagate along the cohesive elements and the exact crack propagation may be simulated if cohesive elements are inserted in all possible directions.

The predicted deformation is similar to that observed in the experimental tests. Figure 4-23 and 4-24 perfectly show the capability of CZM to simulate crack initiation and propagation. These figures show that the horizontal distance of the crack locations match the distance from experimental tests, which were presented in Table 3-2 and Figure 3-21.

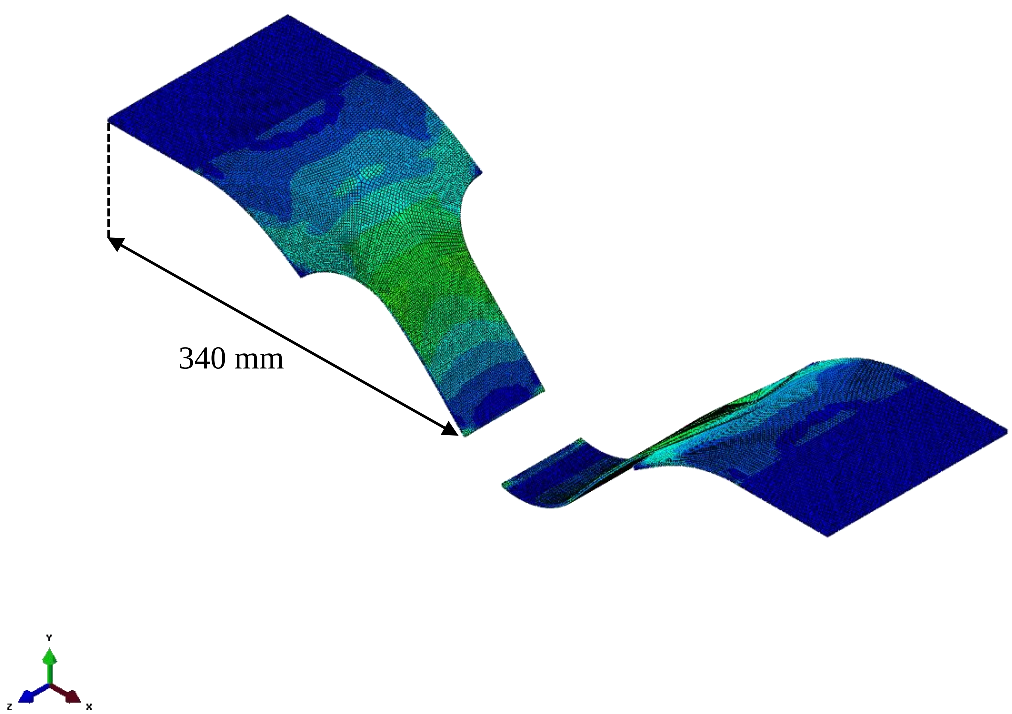

Figure 4-23: Fracture simulation in the thin steel plate

The differences in experimental and numerical horizontal distances can be the result of experimental errors. It should be noted that there is variation in horizontal distances determined from experiments on the specimens with the same dimensions in Table 3-2. Where, the FE model is the idealized simulation of the experiments. Additionally, the position of the cohesive layers and the fact that crack propagate only along the embedded layers affects the crack location.

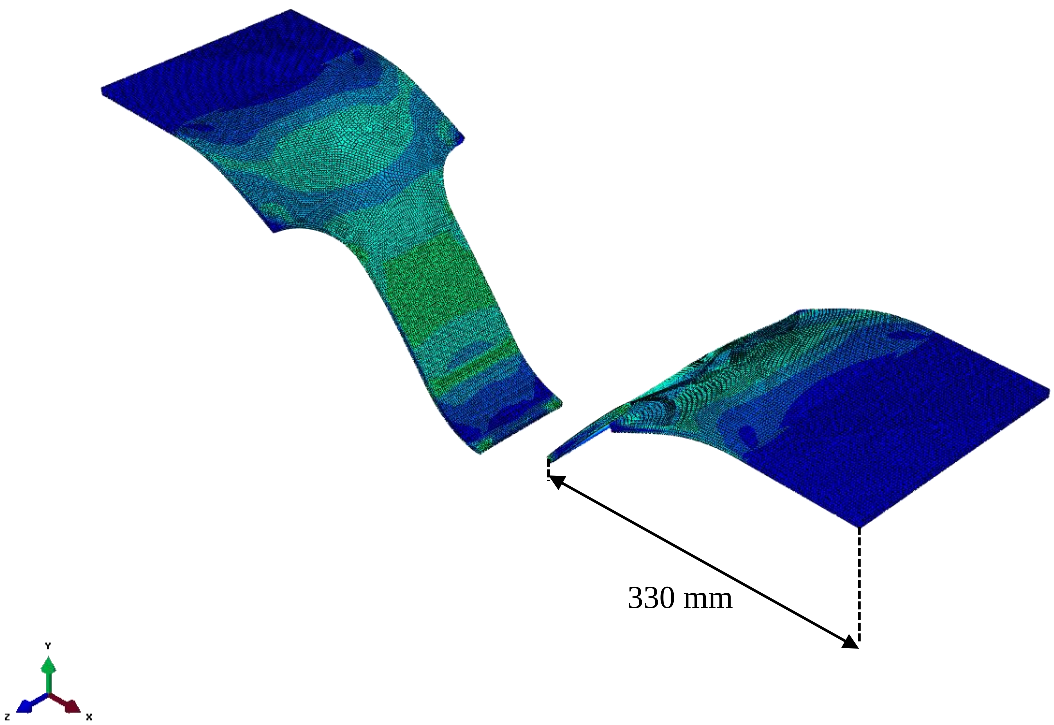

Figure 4-24: Fracture simulation in the thick steel

The force and displacement values of the indenter are recorded during the simulation. The numerical simulation results are compared with experimental results in Figure 4-25 and 4-26. The cohesive model shows very good agreement with the experimental curves. The force-displacement curves show clear transition from plate bending towards membrane behavior. These transition points have some differences with experimental results which can be the result of not having perfectly fixed boundary conditions in the plate fracture experiments. Fracture occurs with an immediate drop in force.

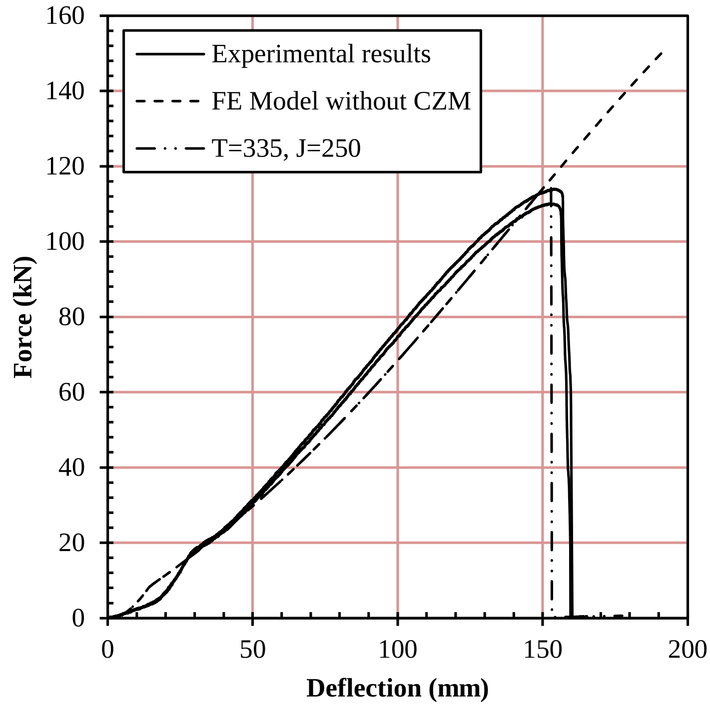

Figure 4-25: Force-deflection curve for the thin plate

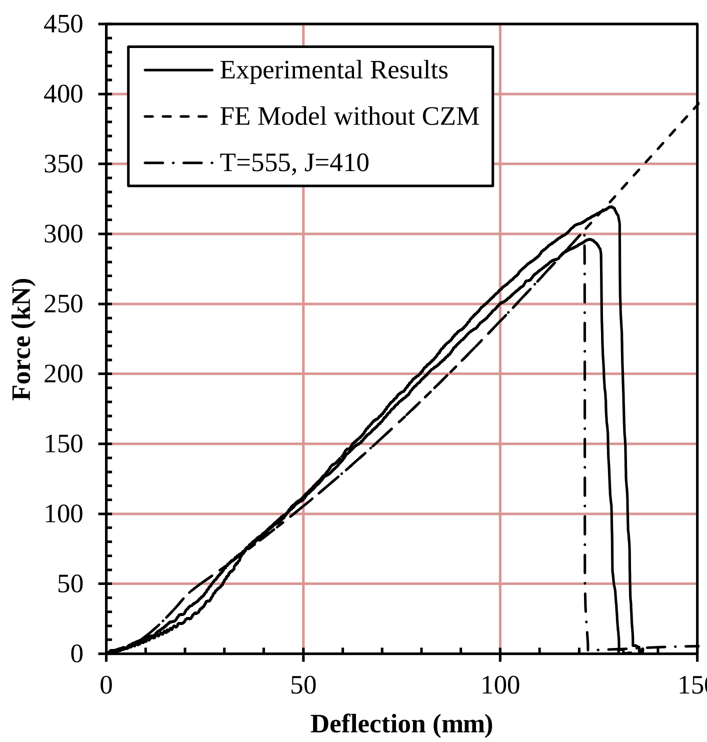

Figure 4-26: Force-deflection curve for the thick plate

One important point for the transferability of the cohesive parameters is that the fracture mechanisms occurring in the steel plate and in the tensile specimen are identical. It is assumed that both structures fail by ductile damage and the fracture surface is flat. Their results showed good agreement between the experimental results and the FEA results when comparing the force-displacement curves. The fact that in numerical simulation, crack starts in the centre and propagate to the surfaces shows high capability of Cohesive Zone Model in simulation of the crack initiation and propagation.

Chapter 5: Conclusions

5-1. Conclusion

To face the new challenges and the extreme ice loads in the Arctic, and to ensure the integrity of structures, structural rupture which are common in ice-structure interactions has been investigated in STePS2 project. The aim of two simultaneous Master theses, as part of STePS2, was to gain a better understanding of the response of steel plates to extreme ice loads by exploring ductile fracture in steel plates both experimentally and numerically. The aim was to develop advanced failure model and to use the results from the experimental tests to provide structural verification data, to insure that the numerical fracture model can simulate the physical fracture happened in the steel plates.

The topic of the current thesis originated to investigate the field of fracture mechanics and related theories and methods. Its main goal was to develop a better understanding of how to use the finite element method to simulate damage and ductile fracture in steel structures. Recently developed method, CZM, was used to simulate crack initiation and propagation numerically.

In order to provide validation data, a test setup and a set of physical experiments have been designed by the other Master thesis (Jamaly, 2014). The experiments address key aspects of the fracture mechanics that the numerical models need to address.

This thesis investigated the cohesive process zone model, a general model which can deal with the nonlinear zone ahead of the crack tip, presents in any kind of material separation. In this thesis, cohesive parameters and the procedure for their determination for simulating normal ductile fracture in steel plates were presented.

A traction-separation law, which describes the constitutive behavior of the cohesive model, was extracted by a method combining experiments and numerical simulation. Cohesive parameters in cohesive zone model, including maximum traction and fracture energy, were determined conducting tensile tests. Then, the tensile tests were simulated numerically to calibrate cohesive parameters. Various combination of T and Γ_0 were used to simulate the tensile tests, and investigating the effect of cohesive parameters. The parameters, that result the best fit of the numerical results to the experimental data, were selected as the final cohesive parameters to model fracture in the steel plates.

Afterwards, the numerical simulation of fracture in the steel plates was conducted to validate the transferability of the CZM. The developed CZM was applied successfully to the steel plates with the same stress constraint and it was shown that CZM is capable of overcoming the disadvantages in using classical Fracture Mechanics or using the damage fracture criteria in numerical simulation. The crack location and the load- deflection curve reasonably compare with the experimental data.

There were no problems, in principle, with transferring the fracture parameters from small specimens to large components. This was one of the big problems in the classical macroscopic fracture mechanics approach.

It was shown that the predicted fracture point depends strongly on the normal cohesive strength. The cohesive energy has only little effect on the fracture estimation. Another parameter influencing the point of crack deviation is the finite element mesh, because the crack can propagate only along the embedded cohesive layers between the continuum elements. However, cohesive elements can be placed between every element faces as a mechanism for allowing all individual elements to separate.

The advantages of the cohesive model can be summarized in the following points:

1. CZM is a phenomenological modeling technique.

   Due to its phenomenological character, the model is adjustable to many different types of materials and failure phenomena. Cohesive laws can be established for various separation phenomena. In summary, the cohesive model can be regarded as a flexible tool for numerical simulation of damage localization and material separation up to structural failure. The classical Fracture Mechanics, LEFM or EPFM, are limited to brittle fracture.

2. The presence of an initial crack is not essential in CZM.

   In this thesis, fracture initiation and propogation in tensile specimens and steel plates were investigated. Notice that these computations could not be done using classical Fracture Mechanics, because no initial cracks were presented in the specimens. Classical Fracture Mechanics Requires a pre-existing flaw at the beginning of the crack surface. It cannot model crack initiation from a surface that is not already cracked.

   On the other hand, CZM can model crack initiation from initially un-cracked surfaces. The crack initiates when the cohesive traction stress exceeds a critical value. The CZM is able to adequately predict the fracture in structures without a pre-existing crack, and not only the response of bodies with initial cracks, which is a common drawback of most fracture models. Therefore, no restrictions exist due to non-existing or non-valid fracture parameters. It was shown that the cohesive model is capable of simulating the ductile fracture in cases where the crack path is not known in advance and the crack was able to evolve anywhere in the specimen that cohesive layers were inserted.

3. CZM is mesh size independent.

   Mesh dependence of numerical results is a big issue in damage mechanics when softening behavior of material is simulated. Since the cohesive law is expressed in terms of stress depending on the separation, a length scale parameter (characteristic length) is inherent to the model. In other words, a cohesive law introduces well-defined fracture energy (fracture or cohesive energy is the work of separation per unit area). Thus, no mesh dependence was expected. It was shown that finite element models with cohesive elements were mesh independent, which is always a big issue in application of fracture criteria in FEA.

5-2. Recommendations for Further Work

The present applications of cohesive models are still far away from practical engineering employment in structural integrity assessments and fracture analysis. There is a strong need to standardize the simulation techniques and the determination of the cohesive parameters. The phenomenological nature of this model is an advantage with respect to its flexibility but may cause some uncertainties about the physics of the underlying processes. Hence, advanced tests and measuring techniques are required for determining the cohesive parameters.

Since CZM is relatively new technique to model the fracture process, there are a lot of topics in CZM that need more investigation and are worth considering. Some are expressed in the following:

1. Cohesive parameters determination

It seems that cohesive laws constitute a research area where modelling is far more advanced than experimental investigations. A few studies cover the determination of the cohesive law. the uniaxial model used, in this study, to derive the cohesive parameters in normal fracture, needs to be generalized to a fully mixed-mode formulation to determine cohesive parameters for other fracture modes. Some other fracture tests may be needed for determining the whole cohesive parameters including tangential parameters.

It must also be noted that the cohesive model is very sensitive to the input data, namely the cohesive parameters. Therefore, the procedures for the determination of the cohesive parameters need further work. New experimental test methods are required for determining cohesive properties and for the calibration of numerical analyses.

2. Investigating the effects of field variables such as stress triaxiality and strain rate effects, to introduce a dependence of the softening function on stress constraint or triaxiality, and/or strain rate.

   Cohesive parameters may depend on the hydrostatic stress state, which is usually normalized by the equivalent stress. This gives the well-known expression for the triaxial stress state, $T = \frac{\sigma_H}{\sigma_{eq}}$. Here, σ_H is the hydrostatic stress and σ_{eq} is the equivalent stress. TSL seems to depend, in general, on the applied stress triaxiality and may depend on other field quantities like loading rate.

   It has been shown by some authors that the cohesive parameters are not material constants, as they may depend on stress triaxiality. However, this dependence may be of second order compared to effects of global plastic constraint (Siegmund, 2000), so that realistic simulations can be performed over a fairly wide range of varying stress triaxiality. (Scheider et al., 2003)

The same issue should be considered for strain-rate effects, so CZM can also be extended to time-dependent material behavior.

3. Developing irregular mesh to simulate arbitrary crack propagation

As mentioned, another parameter influencing the simulation of crack propagation is the finite element mesh. The finite element mesh plays an important role on the crack path and interacts with the effects of the cohesive parameters.

In CZM, since the interface elements are put between the continuum elements of the finite element mesh, the crack propagation in the structure is not totally arbitrary, but can only occur along the element edges of the mesh where cohesive elements are embedded. In order to allow the crack happening everywhere in the structure, a maximum of possible directions has to be provided by the finite element mesh. This is possible by the use of triangular elements in two-dimensional or tetrahedral elements in three-dimensional meshes, respectively.

Another aspect of the mesh issue is the difference between regular and irregular mesh patterns. Since a regular mesh maintains the current direction of crack propagation, it leads to a straight crack path. In the case that the crack has to run through an irregular mesh, the local separation mode in the cohesive elements consists of both normal and tangential separation, where the correct interaction between normal and shear parameters are essential.

In all problems considered in the literature, the crack path was predefined by the location of cohesive elements in a regular mesh, which is actually the real crack path in mode I fracture. However, in general case, a crack propagates in an arbitrary direction. Irregular meshes have the advantage that they do not favor a specific crack-propagation direction. On the other hand, an irregular mesh may make convergence more difficult. In order to simulate arbitrary crack propagation, more experience in FEA and mesh generation for 3D crack growth simulations are needed.

In summary, more powerful computer programs and better knowledge of material properties can definitely increase Cohesive Zone Modeling potential field of application.

References

1. ABAQUS (2010), ABAQUS Documentation, Dassault Systèmes, Providence, RI, USA

2. Anvari, M., Liu, J., Thaulow, C., "Dynamic Ductile Fracture in Aluminum Round Bars: Experiments and Simulations", International Journal of Fracture, 2007; 143:317-332

3. Anvari, M., Scheider, I., Thaulow, C., "Simulation of Dynamic Ductile Crack Growth Using Strain-Rate and Traixiality-Dependent Cohesive Elements:, 2006, Engineering Fracture Mechanics, 2006; 73:2210-2228

4. ASTM Standard E1820, 2013, "Standard Test Method for Measurement of Fracture Toughness," ASTM International, West Conshohocken, PA, 2013, DOI: 10.1520/E1820-13, www.astm.org.

5. Barenblatt, G. I., "The Mathematical Theory of Equilibrium Cracks in Brittle Fracture", Advances in Applied Mechanics, 1962; 7:55-129

6. Benzeggagh, M. L., Kenane, M., "Measurement of Mixed-Mode Delamination Fracture Toughness of Unidirectional Glass/Epoxy Composites with Mixed-Mode Bending Apparatus", Composites Science and Technology, 1996; 56:439-449

7. Carpinteri, A., Cornetti, P., Barpi, F., Valente, S., "Cohesive Crack Model Description of Ductile to Brittle Size-Scale Transition: Dimensional Analysis vs. Renormalization Group Theory", Engineering Fracture Mechanics, 2003; 70:1809-1839

8. Cornec, A., Scheider, I., Schwalbe, K. H., "On the Practical Application of the Cohesive Model", Engineering Fracture Mechanics, 2003; 70:1963-1987

9. Dugdale, D. S., “Yielding of Steel Sheets Containing Slits”, Journal of Mechanics and Physics of Solids, 1960; 8:100-104

10. Elices, M., Guinea, G.V., Gomez, J., Planas, J., “The Cohesive Zone Model: Advantages, Limitations and Challenges”, Engineering Fracture Mechanics, 2002; 69:137-163

11. Gurson, A. L., “Continuum Theory of Ductile Rupture by Void Nucleation and Growth 1. Yield Criteria and Flow Rules for Porous Ductile Media”, Journal of Engineering Materials and Technology, 1977; 99(1):2-15

12. Hillerborg, A., Modeer, M., Petersson, P. E., “Analysis of Crack Formation and Crack Growth in Concrete by Means of Fracture Mechanics and Finite Elements”, Cement Concrete Research, 1976; 6:773-782

13. Irwin, G., “Analysis of Stresses and Strains near the End of a Crack Traversing a Plate”, Journal of Applied Mechanics, 1957; 24:361-364

14. Jamaly, A., Master Thesis, Memorial University of Newfoundland, 2014, in prepration

15. Needleman, A., "A Continuum Model for Void Nucleation by Inclusion Debonding", Journal of Applied Mechanics, 1987; 54(3):525-531

16. Needleman, A., "An Analysis of Decohesion along an Imperfect Interface”, International Journal of Fracture, 1990; 42:21-40

17. Rice, J. R., “A Path Independent Integral and the Approximate Analysis of Strain Concentration by Notches and Cracks”, Journal of Applied Mechanics, 1968; 35:379-386

18. Scheider, I., “Derivation of Separation Laws for Cohesive Models in the Course of Ductile Fracture”, Engineering Fracture Mechanics, 2009; 76:1450-1459

19. Scheider, I., Brocks, W., “Simulation of Cup-Cone Fracture Using the Cohesive Model”, Engineering Fracture Mechanics, 2003; 70:1943-1961

20. Scheider, I., Hachez, F., Brocks, W., “Effect of Cohesive Law and Triaxiality Dependence of Cohesive Parameters in Ductile Tearing”, Fracture of Nano and Engineering Materials and Structures, Springer, 2006; 965-966

21. Scheider, I., Rajendran, M., Banerjee, A., “Comparison of Different Stress-State Dependent Cohesive Zone Models Applied to Thin-Walled Structures”, Engineering Fracture Mechanics, 2011; 78:534-543

22. Schwalbe, K. H., Neale, B., “A Procedure for Determining the Fracture Behaviour of Materials-the Unified Fracture Mechanics Test Method EFAM GTP 94”, Fatigue & Fracture of Engineering Materials & Structures, 1995; 18(4):413-424

23. Siegmund, T., Brocks, W., “A Numerical Study on the Correlation between the Work of Separation and the Dissipation Rate in Ductile Fracture”, Engineering Fracture Mechanics 2000; 67:139-154

24. Tornqvist, R., “Design of Crashworthy Ship Structures”, PhD Thesis, Technical University of Denmark, Maritime Engineering, 2003

25. Tvergaard, V., “On Localization in Ductile Materials Containing Spherical Voids”, International Journal of Fracture, 1982; 18:237-252

26. Tvergaard, V., “Effect of Fibre Debonding in a Whisker-Reinforced Metal”, Material Science and Engineering, 1990; A125:203-213

27. Tvergaard, V., Hutchinson, J. W., “The Relation between Crack Growth Resistance and Fracture Process Parameters in Elastic-Plastic Solids”, Journal of Mechanics and Physics of Solids, 1992; 40:1377-1397

28. Tvergaard, V., Needleman, A., “Analysis of the Cup-Cone Fracture in a Round Tensile Bar”, Acta Metallurgica, 1984; 32: 157-169